# THESIS REPORT

## Master's Degree

## An Investigation of the Mechanics in the Machining of Ceramic Material

*by K.G. Satish*
*Advisor: G.M. Zhang*

**M.S. 94-6**

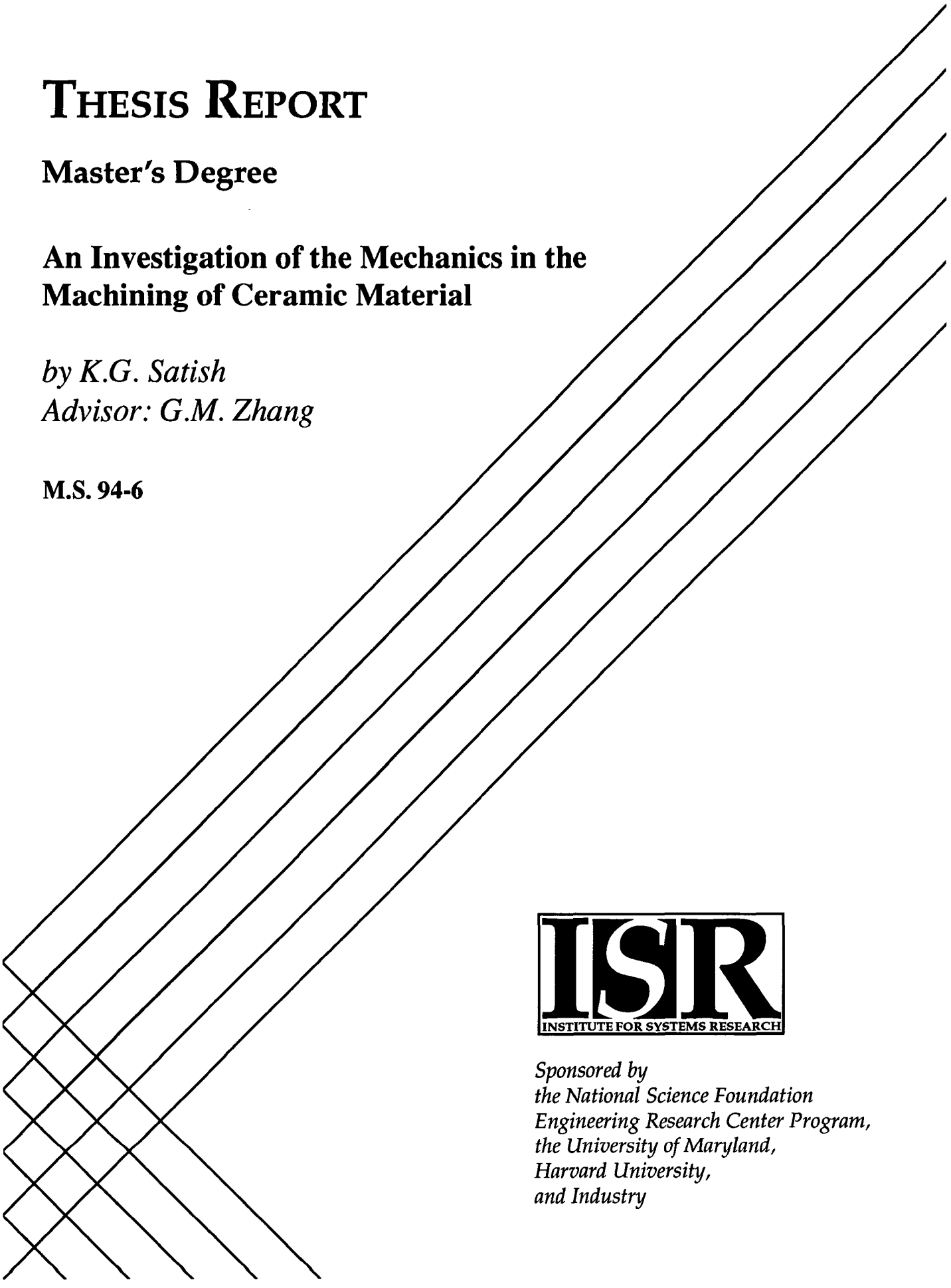




*Sponsored by*
*the National Science Foundation*
*Engineering Research Center Program,*
*the University of Maryland,*
*Harvard University,*
*and Industry*

# An Investigation of the Mechanics in the Machining of Ceramic Material

by

K. G. Satish

Thesis submitted to the Faculty of the Graduate School
of The University of Maryland in partial fulfillment
of the requirements for the degree of
Master of Science
1994

Advisory Committee:

Assistant Professor Guangming Zhang, Chairman/Advisor
Professor Davinder K. Anand
Professor James W. Dally

# Abstract

Title of Thesis: An Investigation of the Mechanics in the Machining of Ceramic Material

Name of degree candidate: K. G. Satish

Degree and year: Master of Science, 1994

Thesis directed by: Assistant Professor Guangming Zhang
Department of Mechanical Engineering
and Institute for Systems Research

This study is an investigation into the mechanics in machining ceramic materials. Extensive experimentation is done in an effort to understand the process of material removal. The theory of fracture mechanics is used to explain experimental findings. A five stage model of the machining of ceramics is proposed, and based on this understanding, guidelines are provided to adapt the traditional methods to machine ceramics. The possibility of developing a new submerged machining process is studied. The significant new findings in this research are:

- Cutting force has little change with increase in the cutting speed as a result of the combined effects of increase in loading rate and increase in temperature on the fracture toughness.
- The quality of the surface formed is better controlled by the variation in the chip size than by the mean of the chip size. Submerged machining creates a unique environment which keeps the chip size variation under control.

- Variation of the chip size increases with increase in the depth of cut, consequently degrading the finish quality. Similar effect of feed has also been observed, however, feed is not as significant as depth of cut.

- The apparent coefficient of friction controls the tensile stress distribution in the vicinity of the cutting zone. A large friction force induces a tensile stress field confined to a narrow region parallel to the machined surface,promoting chip formation.

# Dedication

To my parents

# Acknowledgements

I would like to thank Dr. Guangming Zhang for his guidance and his patience. Without his help, this work would not have been possible. Also, I would like to thank Mr. Wing Ko for his contributions to this work. His energy and enthusiasm have been a constant source of inspiration.

I would like to thank the members of my committee, Dr. Davinder K. Anand, and Dr. James W. Dally, for spending time reviewing my thesis. The completion of this work on time, would have been impossible without the help of Mr. R. Bonenberger. I am grateful for the time and effort that he spent on building the submerged machining apparatus. Finally, I would like to extend my gratitude to all the members of the ADML team for making the lab a good place to work at and Mr. Shuvanker Ghosh and Mr. Rajesh Ratnakar for their guidance through my initial days at the lab.

# Table of Contents

# List of Tables

# List of Figures

# Chapter 1

# Introduction

Ceramic materials are one of a range of new materials that are finding applications in the field of technology. Machining of new materials is an area of research that is vital to realise the complete potential of these materials and, by making them commercially viable, bring them within the access of designers and consumers. An understanding of the behaviour of these materials under traditional machining methods is vital to achieving this objective. This research specifically deals with the processing of ceramic materials. This chapter gives a brief introduction to ceramics and machining processes. Some research needs related to machining new materials are also reviewed here.

## 1.1 Ceramics

Ceramics is defined as the art and science of making and using solid articles which have as their essential component, and are composed, in large part of, inorganic nonmetallic materials [KBU75]. This definition covers both traditional ceramics as well as new ceramics.

Traditional ceramics include pottery, cement, glass etc. These materials can still be seen used in a number of applications today. In spite of its antiquity, the ceramic industry is not stagnant. In the last twenty years, a host of new materials have been developed to serve various purposes. Their engineering applications are of great interest and have opened new fields for research. Many exciting potential applications are still commercially unviable due to a lack of efficient machining processes.

## 1.2 Historic Review of Machining Processes

In the development of any new material, processing the material is a very important aspect, since very often, this forms a substantial fraction of the total cost incurred in making a product. Primary research activities during the past have focussed on improving the characteristics of ceramics with little concern toward machining. In fact most of the information on machining of ceramics deals with the grinding process. Little information on the actual cutting of ceramics, especially on fundamentals of the physics of machining ceramics is available.

The machining of ceramic materials is very difficult due to its hardness. For this reason, it is always desirable to form the ceramic component from the powder into a near net shape. But this is possible only in very few cases. Most of the components are sintered to as close to the net shape as possible and then made to undergo some kind of machining operation to bring it within the required tolerances.

Owing to the difficulty in machining ceramic materials, the processes employed today are mainly those that use abrasion to remove material. Predomi-

nant among these is grinding. Minute cuts are performed to remove material at fast feed rates and cutting speeds. Diamond abrasives are bonded to grinding wheels using different types of bonds. Grinding is useful in this regard since it essentially employs thousands of cutting tools, discarding those that wear out and replacing them with new cutting edges. But the process suffers some significant disadvantages. There is no control over the tool geometries being used in this process since the grains can have any shape and size. Therefore there are many grains that, in the process of material removal, create many microcracks below the surface. This severely limits the strength of the material. Due to this nature of the grinding process, surface integrity of the machined surface suffers. A type of grinding process called creep grinding has been used to grind ceramics. Creep grinding machines the ceramic material by taking the full depth of cut desired and traveling at a creep feed rate. This process has had some success, but is slow as its name implies. This hampers productivity and raises the cost of the equipment used to machine the component.

Turning is a single point cutting process which offers some advantages over the grinding process. Turning allows good control over the cutting tool geometry. In addition, it is possible to achieve higher rates of material removal in turning than in any abrasive process. But due to the high hardness of ceramic material, the rate of tool wear in a single point cutting operation is a cause for concern. Studies are being conducted with an aim to adapting this machining operation to ceramic materials.

Milling is a very important multiple point cutting operation. This operation can give a high material removal rate and offers very good control over tool geometry. Milling is also one of the most versatile machining operations.

Therefore, milling of ceramic materials poses definite advantages over other operations. With the development of machinable ceramics, the scope for milling as a viable machining operation for the processing of ceramic materials, has increased greatly. This research focusses on adapting this machining operation for the purpose of processing ceramic materials.

## 1.3 New Challenges

In the search for better materials and means to use them, three key issues need to be addressed.

- The first is for existing machining technologies to be modified and adapted to machine the new materials as efficiently as possible.
- The second is to use the experience gained with the machining of these materials to develop new processes that can improve the machining performance over traditional methods.
- The third is to design the material microstructure with an aim to improving the machinability of these materials without compromising the advantages in material properties that prompted the development of the material.

In order to process ceramic material efficiently, machining has to be adapted to the specific characteristics of the ceramic material, namely, hardness and brittleness. Demand for understanding material specific removal mechanisms has always existed for developing new and cost-effective machining technologies[KCS+91]. This research addresses the first two issues by attempting to gain an understanding of the material removal mechanism specific to ceramic

materials and using this knowledge to adapt traditional machining methods to the machining of ceramic materials. A new process designed to improve upon existing machining methods is proposed and studied.

## 1.4 Objectives of this Research

This research is concerned with the adaptation of existing technology to process ceramics and with the development of a new process to improve upon the existing ones. Information on the material removal mechanism during the machining of ceramics is obtained through extensive experimentation. This is used to adapt the traditional process of milling to machine ceramic materials more efficiently by providing guidelines. In addition, a new process based on the effect of environment during the machining process is proposed and studied for an improvement in machining performance.

The thesis is organized into six chapters. The first chapter "Introduction" has provided a brief review of ceramic materials and machining processes.

The second chapter "Background and Literature Survey" gives an introduction to the properties of ceramic materials and some issues in conventional machining. This chapter also deals with the work done in related topics in the past and seeks to comment on their use and relevance to this work.

The third chapter "Investigation of the Material Removal Mechanisms" lays the theoretical basis for an understanding of the material removal mechanisms in the machining of ceramics. This chapter builds upon the past experience with research in ceramic machining.

The fourth chapter "Experimental Setup" deals with the designing and fab-

rication of certain equipment required for this study. There is also a brief introduction to instruments, like the Environmental Scanning Electron Microscope, which are used in performing experiments.

The fifth chapter "Experimental Study of Ceramic Machining" lists in detail the procedures used to perform the experiments and the results obtained from these experiments.

In the sixth chapter "Discussions of Results", the results of experimentation are used to get a deeper understanding of the processes involved during the machining of ceramics.

The seventh and final chapter "Conclusions and Future Work" summarizes the work in the form of some conclusions and also lists possible future directions for research.

# Chapter 2

# Background and Literature Survey

This chapter reviews briefly the properties of ceramic materials and the issues involved in the machining of ceramics. A literature review of these fields is presented in the final two sections of this chapter.

## 2.1 Importance of Ceramic Materials

Since the industrial revolution, engineers have always sought to develop new and innovative solutions to engineering problems and to provide opportunities for product developers to improve and renovate the existing products. For example, every design engineer has to operate within certain constraints and one of the most formidable of these constraints is the material properties. A new material with an improved desirable property therefore opens new ways of improving existing designs and can offer very great potential for improvement. Material scientists have, for years, been trying to improve such properties of materials as

strength , heat resistance, hardness etc. This has led to the development of advanced ceramics. Since the first use of ceramics by man many centuries ago, the techniques of developing ceramic materials and the number of specialized materials falling in this category have increased tremendously. Today, industries such as aircraft, automotive and micro-electronics are finding increasing applications for ceramic materials.

As the demand for new and better properties has led to the development of new materials, the availability of new materials has led to new uses based on their unique properties. For example, ceramics are now being used as magnetic ceramic materials. Some of these materials have a very nearly square hysteresis loop that is most desirable for computer memory circuits. Ceramic materials are now being developed for use as smart materials and actuators with a wide range of applications. In rocketry and missile development, the nose cone and the rocket throat are made of ceramic materials since these components have to withstand very high temperatures. Uranium oxide (urania) is now used in nuclear reactors. In 1990, the advanced ceramics industry in the United States consisted of approximately 100 different companies with sales equal to about 14 billion dollars per year and a growth rate of 8% per year[EW90]. Thus the relevance of ceramics to modern technology has increased over the past few decades and there is an urgent need to understand the basic mechanisms in the making of ceramic materials and in manufacturing structural components from them. There is also the need to improve traditional methods or develop non-traditional methods of machining ceramics to achieve their full potential.

## 2.2 Properties of Ceramic Materials

This section presents a review of the properties of ceramic materials. Many terms related to metals have been used. In most cases, these mean the same when applied to ceramics too. However, under certain circumstances, the terms may not imply the same results as in the case of metals. These differences will be pointed out when they are encountered. 2.1 shows a comparison of the important mechanical properties of four different ceramic materials. In this table, $HP - Si_3N_4$ stands for hot-presses silicon nitride, $HP - SiC$ stands for hot-pressed silicon carbide and $PSZ$ stands for partially stabilized zirconia.

1. Strength:

In metals, strength in general refers to the yield strength. Beyond this point, a ductile material starts yielding and this usually means the failure of the component. In ceramics, the load required to achieve significant deformation can be more than that required to fracture the material. This load is more in compression than in tension. The strength of the material is affected by grain size, porosity, flaws etc. Increasing the grain size reduces the strength.

Griffith[A.A20] proposed an equation of the form

$$\sigma_f = A(\frac{E\gamma}{c})^{1/2}$$

for relating the fracture stress to the material properties and flaw size where $\sigma_f$ is the fracture stress, $E$ the elastic modulus, $\gamma$ the fracture energy, $c$ the flaw size and $A$ is a constant that depends on the specimen and flaw geometries. Evans and Tappin[A.G79] have presented a more general relationship.

$$\sigma_f = \frac{Z}{Y}(\frac{2E\gamma}{c})^{1/2}$$

| Property | | Material | | | |
|---|---|---|---|---|---|
| Name | Units | $Al_2O_3$ | $HP-Si_3N_4$ | $HP-SiC$ | $PSZ$ |
| Specific Gravity | | 3.98 | 3.17 | 3.22 | 6.27 |
| Melting Point | $^oC$ | 2050 | 1900 | 2220 | 2715 |
| Hardness(Hk) | $kg/mm^2$ | 1150 | 1460 | 1880 | |
| Fracture Toughness | $MPa.\sqrt{m}$ | 4.0 | 5.0 | 4.0 | 7.6 |
| Modulus of Elasticity | $GPa$ | 380 | | 414 | 138 |
| Compressive Strength at Room Temp. | $kg/cm^2$ | 2800 to 3500 | 5000 to 8000 | 6000 to 42000 | 10000 to 30000 |
| Bending Strength at Room Temp. | $kg/cm^2$ | 3000 to 4000 | 5000 to 10000 | 4500 to 8000 | 1800 to 8000 |

Table 2.1: Comparison of Properties

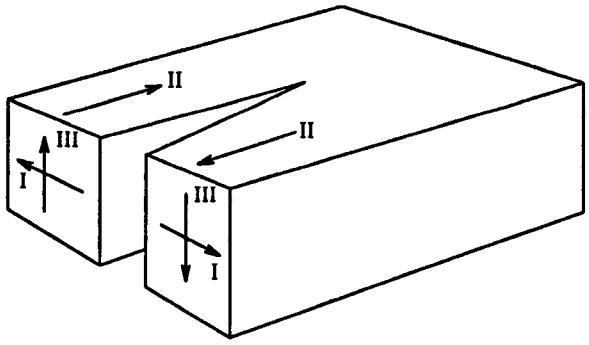


Figure 2.1: Modes of Loading

where $Y$ is a dimensionless term that depends on the flaw depth and the test geometry, $Z$ is another dimensionless term that depends on the flaw configuration and $c$ is the depth of the surface flaw.

2. Fracture Toughness:

Another approach considers fracture in terms of crack surface displacement and the stresses at the crack tip. The stress concentration at a crack tip is denoted in terms of the stress intensity factors $K_I$,$K_{II}$ and $K_{III}$ where the subscripts refer to the mode of loading as shown in figure 2.1. Mode I is most frequently encountered in ceramic materials. The fracture toughness is defined as that stress intensity factor at which the crack will propagate and lead to fracture. This is also called the critical stress intensity and is denoted by $K_{IC}$. This is a property of the material but can vary with temperature and the loading rate. The higher the fracture toughness of a material, the more difficult it is to propagate a crack in that material. The mode $I$ stress intensity factor is related to other parameters by the following equations[HC93]

For plane strain,

$$K_I = (\frac{2\gamma E}{1-\nu^2})^{1/2}$$

For plane stress,

$$K_I = (2\gamma E)^{1/2}$$

where $\gamma$ is the fracture energy, $E$ the elastic modulus and $\nu$ is Poisson's ratio.

3. Thermal:

One of the most desired properties of ceramics is its thermal properties. Ceramics are known to withstand service temperatures up to $3000^o F$ [Adv89]. Ceramics also have much better hot hardness than metals. These properties make them suitable for high temperature and refractory applications. In addition, the coefficient of thermal expansion for ceramics is considerably smaller than for metals. However, the thermal shock resistance which is the ability of a material to withstand thermal stresses due to large temperature gradients is low in brittle material. In some applications, this restricts the use of ceramics [Adv89].

4. Hardness:

Hardness is the ability to resist wear and abrasion. The hardest materials known today fall in the category of ceramics. This particular property is very desirable in certain applications. In particular, in the metal cutting industry, ceramic cutting tools are used in the form of inserts to cut other hard materials.

## 2.3 Issues in the Machining of Conventional Materials

Since many decades, models for the machining of ductile materials have been developed and though some issues remain unresolved, the models existing for

ductile materials have been far more successful than those for brittle materials. To contrast with the research concerns related to the machining of brittle materials, a brief review of the basic issues involved in machining ductile materials is presented in this section.

It is now well accepted that machining in ductile materials takes place by shearing the material, causing plastic flow over the rake face of the tool. The tool applies a force on the flowing material thus moving forward and removing the material. The material flowing over the rake face applies a load on the tool due to friction. This causes the microstructure of the chip to change drastically and the chip curls in most cases and breaks off at regular intervals. The form of the chip produced is thus a valuable indicator of the processes occurring at the tool-chip interface.

The forces at the tool-workpiece interface are dynamic in nature due to the stiffness of the machining system and the variations in properties of the workpiece. This causes the tool to vibrate and under particular conditions can set the system into a condition of instability. In other cases, the vibration is revealed as the variations in surface topography produced and many attempts have been made to improve surface finish through the attenuation of vibration.

The tribological interactions occurring at the machining interface are an important field of study. Much work has been done on the effects of parameters like the cutting conditions and the choice of cutting fluids on these interactions. It has been recognized that the lubricating effect due to the application of cutting fluids manifests as a decrease in the length of chip in contact with the rake face of the cutting tool. It has been confirmed that the effectiveness of cutting fluids is through a combination of cooling the cutting zone, removing the machined

debris from the cutting site and lubricating the flow of chips over the rake face of the cutting tool. Lubrication is a complex phenomenon and many mechanisms are believed to be involved in the process.

## 2.4 Fundamental Research in the Machining of Ceramics

This section provides a review of fundamental research relevant to this study. The goal of fundamental research is to study and explain the processes that take place during the machining of ceramics. Though many theories of machining have been developed earlier, most of them were modeled on machining metals and ductile materials. It has been realised since, that the theories have to be radically modified to explain the observations made in the case of ceramic materials.

The pioneering work towards understanding the basic mechanisms of ceramic machining considered the grinding process as being representative of the cutting mechanisms involved in ceramic machining. The indentation fracture mechanics approach has been used to study the chipping mechanisms in grinding. This approach assumes that the damage produced by grinding can be modeled as an idealized crack system produced by a sharp indenter. Evans and Marshall[EM80], using this approach, concluded that the cutting mechanisms are due to plastic flow and lateral cracking. They have predicted a lateral fracture threshold loading limit below which plastic cutting occurs. But on crossing the threshold, lateral cracking occurs.

Figure 2.2 shows the cutting mechanisms involved in the grinding process. Kirchner and Conway[KC85] indicated that the cutting mechanism of the single

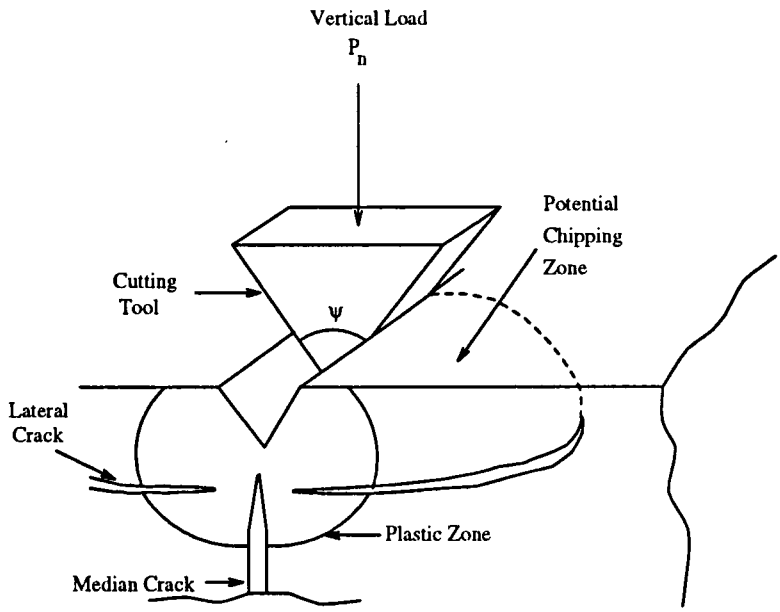


Figure 2.2: Mechanisms of Cutting [EM80]

point grinding of ceramics may include factors such as friction cracking, plastic flow crushing, elastic recovery, generation of residual stresses, radial cracking, lateral cracking , chipping and strength degradation. The occurrence of specific factors for cutting mechanisms is dependent upon the type of loading condition. They observed that friction cracking, perpendicular to the cutting groove is caused by the frictional forces in the wake of the tool fracturing the material in tension. Unlike in ductile materials, the principal mechanisms of material removal are crushing and chipping.

Research of fracture mechanics over the last few decades has provided strong evidence that cleavage fracture is the most common fracture mode of ceramic materials when they are being machined[Bat89, Law75, CC91]. The interplay between the dynamic characteristics of a machining process and the micromechanisms and metallurgical aspects of fracture mechanics calls for a systematic study of the physics behind the material removal process during machining.

Evans and Marshall[EM80] have assumed that the tool traveling across the workpiece surface acts like an indenter to compress the material, thus inducing compressive stress and forming three deformation zones. As the compressive stress builds up in the cutting zone, crushing and chipping are produced by brittle fracturing through stress wave propagation. It has been seen in previous work that the fracture strength of a brittle material fluctuates. This fluctuation can be as much as an order of magnitude[Law75]. This fluctuation can cause a large variation in cutting forces and correspondingly increase impact on the material.

Lawn[Law75] and Landes[LH89] have studied the fracture process in brittle materials and confirm the existence of deformation mode of fracture. The elastic-plastic fracture mechanics may be applied to characterize the crack tip field in the chip formation process. Zhang et.al[ZAGK93] have confirmed that there is plastic flow over the rake face before separation into chips occurs due to cracking. The specific grinding energy for chip formation through fracture was also observed[HM76] to be an order of magnitude lower than that for a plastic mode of chip formation. Hence, fracture became the predominant chip formation mechanism at larger depths of cut.

Studies have been conducted on the environmental effects at the cutting zone. The tribological interactions on the interfaces between the cutting tool and ceramic material have a strong effect on the cutting mechanism[Kra91, ZHAJ92]. It has been observed that the feed cutting force increases while the tangential cutting force decreases when a selected chemical additive is added to distilled water. In fact water has been found to exhibit significant effects on the tribological behaviour of alumina[GHK89]. A film-like substance has been found on

the surfaces of water lubricated alumina wear surfaces, suggesting the possibility of tribological reaction between water and alumina in the contact junction. It has been found that at high temperature(about $200^oC$) aluminum oxide hydroxide(boehmite, $AlO(OH)$) is formed, while at lower temperature (about $100^oC$) the formation of aluminum trihydroxide(bayerite, $Al(OH)_3$) is favored.

Use of cutting fluids can improve machining efficiency. In the study of environmental effects on fracture mechanics, stress - corrosion cracking was found to cause intergranular or cleavage separation by a loss of cohesion [Ger89]. Chemical - assisted machining has been studied intensively showing great promise for enhancing machining performance[ZHAJ92].

## 2.5 Development of New Machining Processes

The theories established through fundamental research have been applied to develop new processes or modify old ones to achieve faster and better machining of ceramic materials. This section gives a brief review of applied research in the field of machining of ceramic materials.

Research in this field has focussed on abrasive processes as an effective method to machine ceramic materials. With the availability of abrasive grains consistently to high levels of performance and dimensional accuracy, the grinding process has maintained its popularity in machining ceramics[SRM90]. But all abrasive methods suffer from one significant limitation, i.e., the lack of control over cutting tool geometry. Due to this factor, surface and subsurface damage is inevitable and this severely limits the quality of the component. Some studies have been conducted to implement abrasive jet machining to cut ceramic ma-

terials. In abrasive jet machining, the high pressure abrasives wash and pierce ceramic materials away[Maz91]. But abrasive jet machining again suffers from the same limitation as all abrasive processes. In addition, the availability of advanced equipment and economic factors have limited its use on the shop floor.

To study the issue of strength degradation of the finished part due to surface and sub-surface damage, the chip formation process has been modeled as a system of radial and lateral cracks[HC93]. It was observed that the effective bulk modulus of the workpiece layer near the free surface can be reduced substantially by introducing appropriate distributions of microcracks. Attempts are being made to design and incorporate a microcrack distribution in the workpiece that would improve the machinability and reduce surface and sub-surface damage.

Recently, a new method "heat assisted machining" which integrates laser machining and grinding, is being developed. By grinding ceramic materials in a ductile regime, quality and productivity could be significantly improved.

Grinding wheels made of hard structural ceramic materials such as $Si_3N_4$, $SiC$ and alumina(hot pressed silicon nitride ceramics) are capable of achieving high quality of microfinishing. It was reported that the roughness average value ($R_a$) of the surface ground by wheels of no.140-200 mesh size diamond abrasive was about 0.1 to 2 micrometers[16].

As reported in [CJW86], a "laser lathe" was developed where the dual beam principle was applied to remove ceramic materials in a molten form. This process eliminates vibration since it is a non-contact type of machining. But ceramics have very poor thermal shock resistance. This means that large temperature gradients can cause the brittle material to develop cracks. Coupled with the

fact that the melting temperatures for ceramics are in general higher than most metals, damage due to thermal shock is unavoidable. The surface and sub-surface damage thus induced are the drawbacks of the technique.

# Chapter 3

# Investigation of the Material Removal Mechanisms

This chapter presents an investigation into the mechanics of material removal in ceramic materials during machining. A model for machining ceramics is proposed and some implications are considered.

## 3.1 Analysis of Machining Mechanisms

In this research, the theory of fracture mechanics has been used to gain a basic understanding of the mechanics of the material removal process during the machining of ceramic materials. Characteristics of the fracture of brittle solids have been used to predict the modes of material removal and some implications have been considered.

The material removal mechanism observed during the machining of metals indicates that whenever a cutting tool cuts into the workpiece material, elastic deformation begins and three deformation zones are formed as stress builds up

in the material. In the machining of aluminum oxide, the presence of chips, the formation of surface texture, and the tool wear observed on rake and flank faces support the existence of the three deformation zones[ZSK94]. However, the variation in the sizes of chips and its correlation with surface finish are phenomena that are not observed in the machining of ductile materials. Furthermore, it has been observed in machining ceramic materials that the final depth of cut is usually more than the desired depth of cut[LCK85]. In machining ductile materials, elastic recovery causes the final depth of cut to be smaller than the desired depth of cut. This indicates that the amount of elastic-plastic deformation is much smaller in the case of ceramic materials. Therefore, the material removal process during the machining of ceramics cannot be simply explained based on the metal cutting principles. There must exist some mechanism or mechanisms during the machining of ceramic materials that are different from those observed during the machining of conventional materials like metals.

The ceramic material, being a brittle solid, has its inherent fracture toughness. It has been known that the fracture toughness can decrease significantly with increasing loading rate. Figure 3.1 presents a comparison of two fracture toughness curves obtained under two different loading rates, indicating the tendency of decreasing fracture toughness as the loading rate increases. In the machining of ceramic material, machining at a high cutting speed is equivalent to applying a load at a high rate. Consequently, the inherent fracture toughness of the ceramic workpiece decreases significantly. Fracture replaces shearing as the prevailing mechanism in the material removal process. On the other hand, the temperature of the material at the interface with the rake face increases due to friction. This causes an increased toughness on that interface. As a result

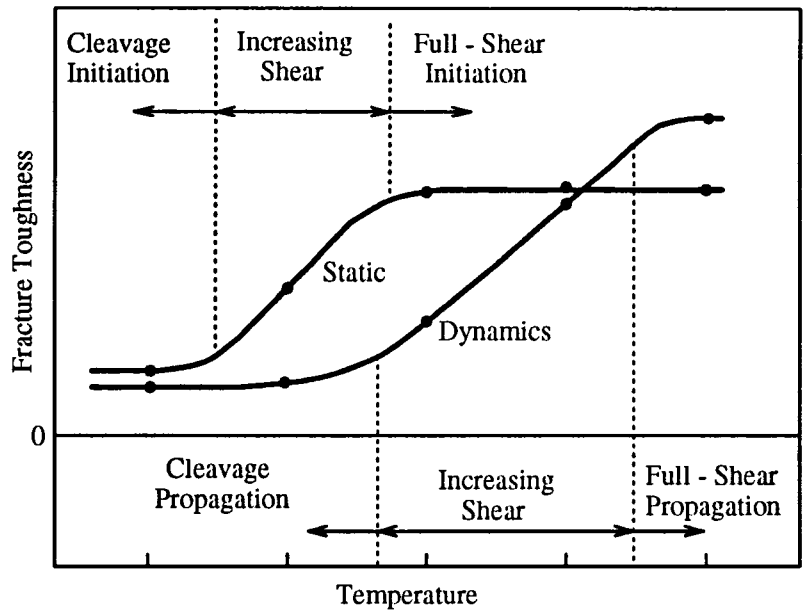


Figure 3.1: Variation of Fracture Toughness with Temperature[BR87]

of the low thermal conductivity of the ceramic material however, the effect of high loading rate predominates in the rest of the material. Thus, any plastic deformation that might occur is restricted to this interface. The predominant mode of failure is therefore brittle fracture that occurs through the body of the workpiece. Chip formation is only due to a fracture process characterized by crack initiation, propagation and cleavage.

Adams and Sines[AS76] have presented extensive evidence of fracture originating from distributed flaws in contact stress fields in glass. Possible mechanisms of material removal may therefore involve initiation of cracks at origins distributed throughout the stressed volume, coupled with sufficient interaction among the cracks, to cause intersection of the cracks and separation of particles. Increased interaction among cracks could result from the local instabilities caused by the changes in the stress distributions in response to cracking. Even in those materials where multiple crack initiation origins are not present, crack branching

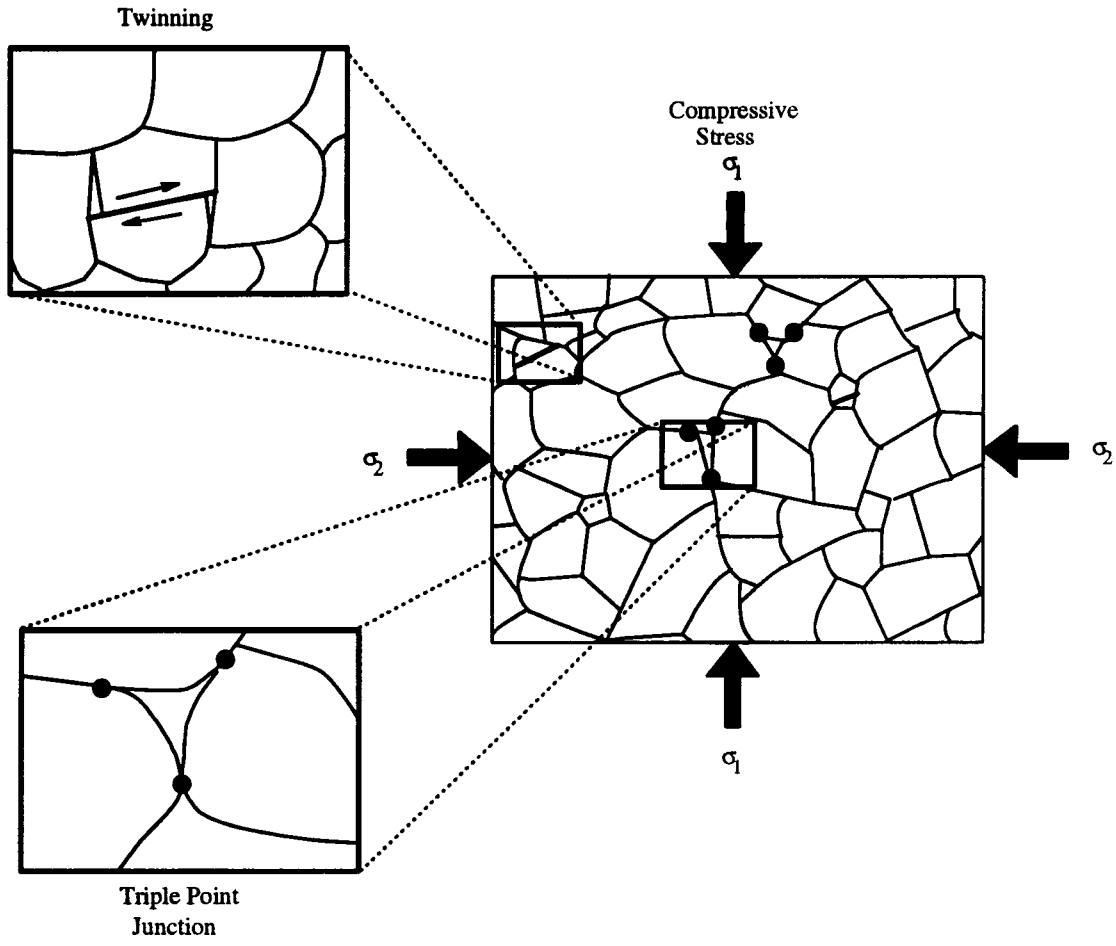


Figure 3.2: Types of Microstructural Discontinuities

can ensure that the stressed volume separates into many small particles.

Crack initiation sites or "fracture origins" can be one of many different discontinuities in the microstructure of the material. Two of the most common types of discontinuities are shown in the figure 3.2. The triple point junction is formed at the junction of three different grains. This configuration creates three vertices of very high stress concentration. As the stress intensity factor rises, a crack is initiated at one of the three points. The crack propagates preferentially along the boundary of the grain since transgranular cracks, though possible, are less likely than intergranular cracks. All the strain energy stored in that region is relieved through the propagation of the crack. This prevents the initiation of a crack close to that region. Similarly, cracks formed due to intergrain shear faults or twins, can act as crack nucleation sites. Twinning is the result of extremely localized plastic deformation in the microstructure, along the plane of maximum shear stress. Removal of material can therefore occur in the form of single or multiple grains. Fractional grains are also possible, but can be expected to be fewer in number due to the relative improbability of a transgranular crack.

## 3.2 Analysis of Stress Distribution

When the tool touches the workpiece, an elastic stress field is established. The nature of this field can give valuable information on the micromechanisms of failure that follow. To study this, a finite element analysis using a linear elastic material was undertaken. Such an analysis is applicable to advanced structural ceramics, which are brittle, since they adhere to Hooke's law. In the machining process, the cutting tool applies a load on the surface of the workpiece while

moving relative to it. This causes an additional friction load at the interface between the rake face of the tool and the workpiece. The tangential load depends on the cutting parameters and the environmental conditions present at the interface. To study the effect of this friction loading, the two extreme cases of no friction and large friction are considered.

In the case of loading without friction, the resultant force acts normal to the surface of the workpiece. This resembles Hertzian indentation which involves a normal contact load between a sphere and a flat surface. Within the contact circle, the stress field becomes largely compressive, while outside this region, the tensile stress in the surface drops off as the radial distance from the center of contact increases. Below the surface and outside the contact area, the component of tensile stress diminishes with depth. A tensile "skin" layer thus formed affords highly favorable conditions for crack initiation. In addition, the stress distribution is symmetric owing to the loading symmetry. Though the tensile stress drops off with depth, there is significant stress buildup in the sub-surface layers of the workpiece material.

In the alternate case of loading with a large friction coefficient, the resulting stress distribution is highly skewed as can be expected from the asymmetric loading condition. In the particular case of machining, the direction of the friction force is determined by the direction of motion of the cutting tool. The tensile stresses set up on the surface reach very high values. This is once again a favorable state for crack nucleation. This is supported by the development of the partial cone crack seen in scratch tests on brittle materials. But as a result of the skewed stress distribution, it can be seen that the tensile stress decreases rapidly with increasing depth in the workpiece.

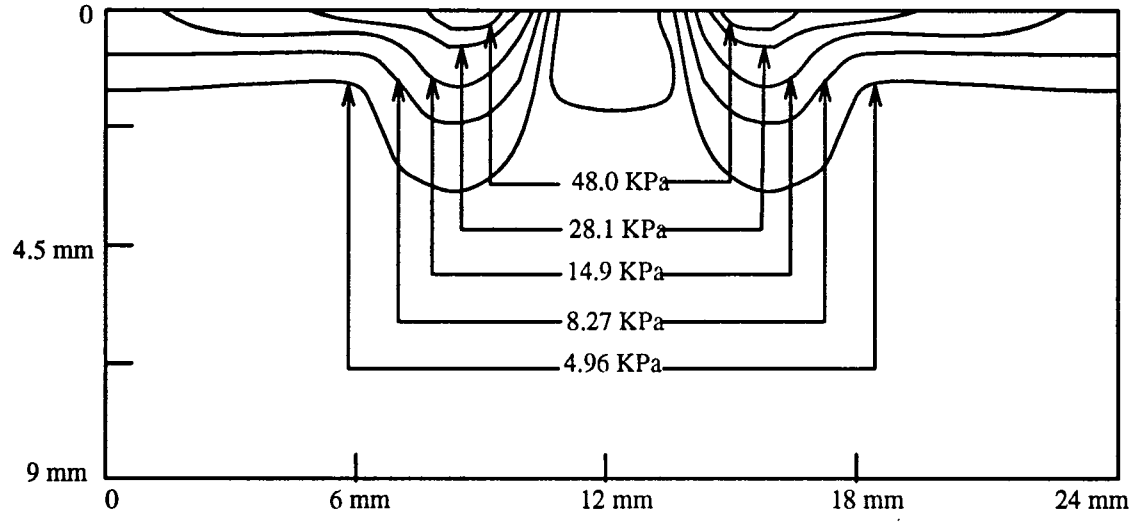


Figure 3.3: Tensile Stress Distribution for Loading without Friction

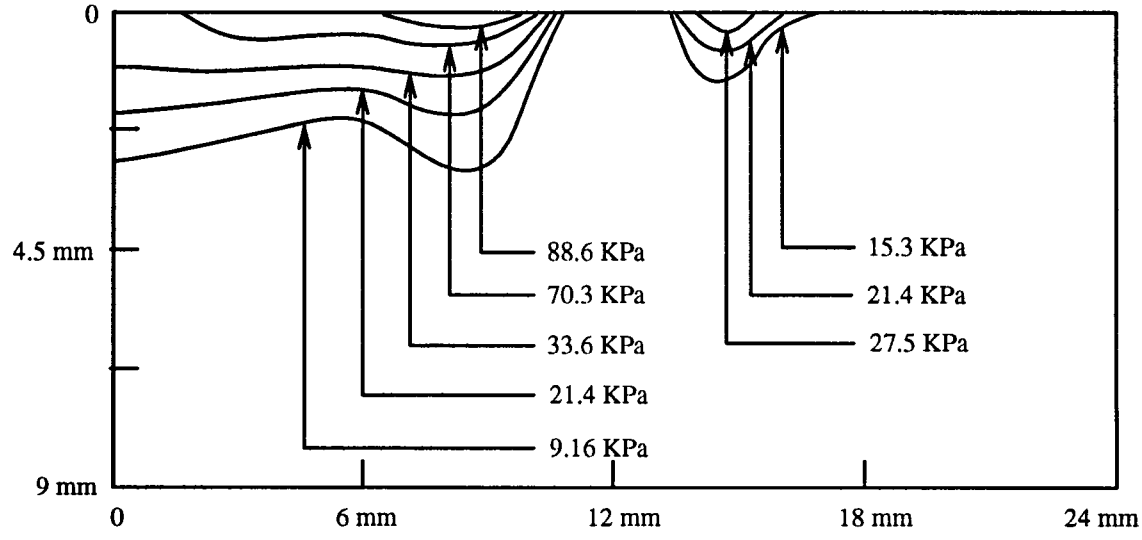


Figure 3.4: Tensile Stress Distribution for Loading with Friction

In a brittle workpiece, it is reasonable to expect a number of flaws that can act as crack nucleation sites within the material. As the stress field increases, it is desirable to restrict the formation of micro-cracks to the uppermost layer. When the friction force experienced is very low, a large normal load is needed to initiate fracture and remove material. With the presence of friction force, the high tensile stresses can be constrained to the top layers of the material, thereby controlling and reducing the occurrence of micro-crack formation in the sub-surface of the workpiece. It is important to note that since a linear elastic material has been used for this analysis, it is only valid for a study of crack initiation and not for crack propagation. Crack propagation, in most cases needs more energy and the moving tool can be expected to provide the energy needed for this process.

## 3.3 Stress Intensity Factor and Fracture Toughness

In this section, the stress analysis of the previous section is coupled with a study of the transition from brittle fracture to elastic-plastic deformation to develop the concept of the idealized microcrack-controlled machining process.

As shown in the previous section, the stress distribution in the workpiece can be controlled through the loading conditions. The purpose of crack-controlled machining is to be able to control the occurrence of brittle fracture and limit it to the layers that comprise the depth of cut. Any further penetration is undesirable and can be detrimental to the quality of the finished component. The stress distribution can play an important role in performing crack- controlled machining.

Any crack propagation process can be viewed as a competition between the stress intensity factor created by the stress field and the fracture toughness of the material under given conditions of loading rate and temperature. Conway et.al [CK86] have studied the variation of stress intensity factor with depth in a specimen subjected to a normal load. In their study, the material was assumed to have a randomly distributed flaw population. A typical result is shown in figure 3.5. The values shown in the figure correspond to hot-pressed silicon carbide. At the point that the stress intensity factor falls below the critical value $K_{IC}$, the fracture mode is no longer brittle. It can hence be expected that there will be little or no sub-surface damage below this depth. On the other hand, there is extensive brittle fracture in the layers above the critical depth causing a deeper depth of cut than desired. Crack controlled machining involves achieving control of this curve with the aid of external independent variables like the cutting parameters and the environmental conditions, to minimize sub-surface damage due to formation and propagation of micro-cracks and the build up of residual stresses that can induce crack propagation during service. Control of factors that influence the shape of tensile stress field induced is essential to achieve this objective.

## 3.4 Model of Machining Mechanisms

From the above discussion, a model to describe the mechanics of material removal during the machining of ceramic material is proposed. This lays emphasis on the relationships between the macroscopic and microscopic fracture behaviours. Figure 3.7 illustrates the five essential stages in this basic physical process:

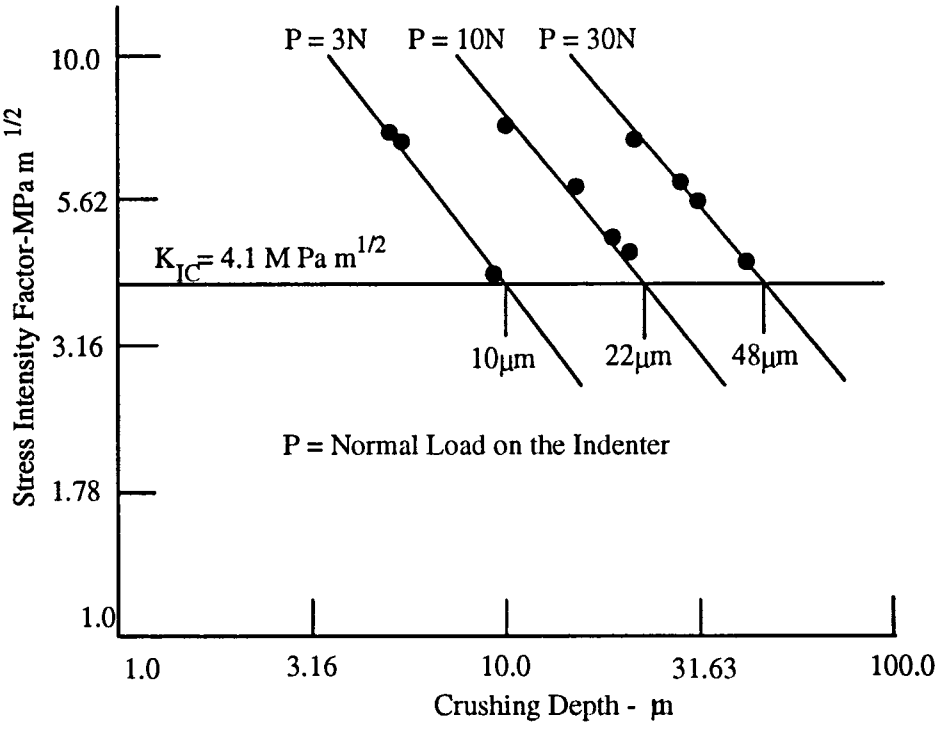


Figure 3.5: Mode I Stress Intensity Factor Variation with Depth[CK86]

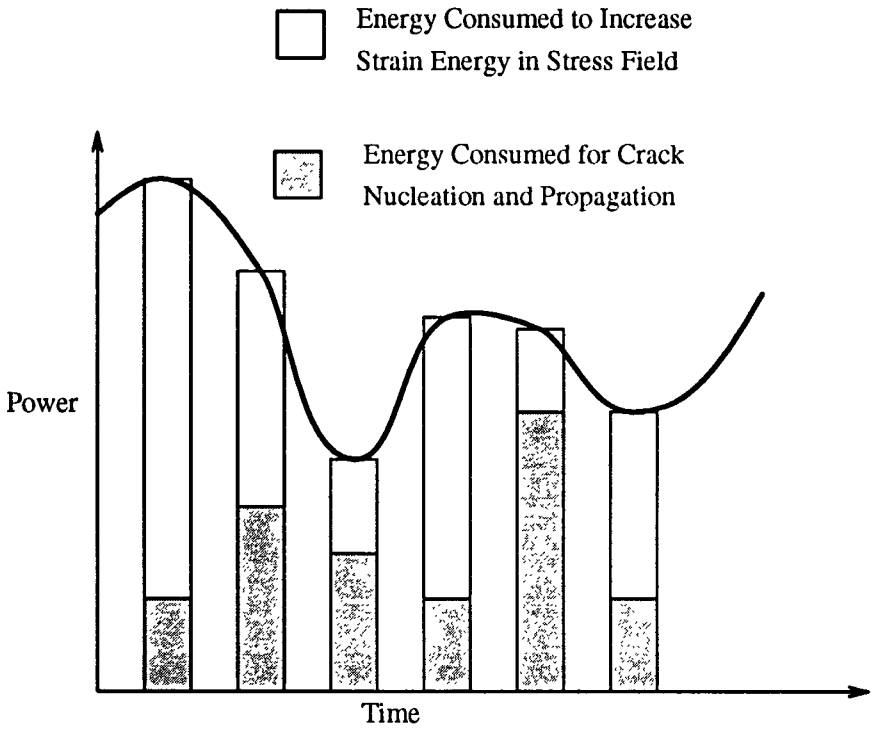


Figure 3.6: Typical Power Variation with Time

- Dynamic Loading: The tool approaches the part material at the beginning. The machining process begins when the tool touches the part material and the impact between them induces stresses in the material. The stresses form a stress field inside the workpiece (figure 3.7a). As the tool moves continuously, the forces on the workpiece material continually change. This causes the loading to be dynamic in nature.

- Strain Energy Built-up and Crack Initiation: The stress field creates regions of hydrostatic stress where the strain energy is stored in a delicately balanced stress system. The strain energy stored in the workpiece material accumulates as the cutting tool continues its movement, especially in locations where the hydrostatic pressure is very high. The induced stresses initiate crack nucleation. The crack sites are locations of stress singularities where high internal tensile stresses accumulate. These locations can be triple-point junctions, dislocation pile-ups at grain boundaries, and second-phase particles. All these discontinuities act as potential sites for the initiation of micro-cracks (figure 3.7b). In a material with a significant flaw density, it is reasonable to assume multiple crack nucleation points. This is especially true for an inhomogenous material like Dicor/MGC.

- Crack Propagation: As the machining process progresses and stresses continue to develop in the material, the formed microcracks propagate through the immediate, surrounding material. Both intergranular and transgranular cracks develop. Obstacles are encountered as the crack propagation advances (figure 3.7c).

- Strain Energy Release and Chip Formation: The process of crack propagation is terminated when more micro-cracks merge and form chip fragments. The generation of new surfaces during the crack propagation creates unique opportunities to release the accumulation of strain energy. The stress field around the propagating crack tip is severely distorted and this destroys the stress balance in these regions causing a release in strain energy. Its sudden release usually leads to catastrophic failure, resembling a micro-scale explosion and promoting crack propagation. The size of particles formed in the catastrophic failure mode depends on the strain energy stored in unit volume in the stress field. Consequently, in the chip formation process, the material separated by fracture can be in a position either contacting the rake face of the cutting tool or positioned away from the cutting zone, depending on the pattern of stress distribution. Two types of chip are formed as a result. The type of machined chip (shadow areas) represents the fractured material directly beneath the tool action, and is also subjected to the influences of temperature. On the other hand, fractured chip type is governed by the stress distribution and the material microstructure (figure 3.7d).

- Formation of Surface and Sub-surface Damage: Chip fragments are formed during machining due to brittle fracture. This causes concurrent formation of cracks in the surface texture of the machined surface. Moreover, some cracks terminate in the solid when crack arrest takes place. These cracks are called surface damage and are, in general, unavoidable during machining of ceramic materials. In addition, the residual effects of brittle fracture near the surface layer bury numerous micro-cracks to a certain

depth, which leads to sub-surface damage (figure 3.7e).

The mechanism described above can be used to understand the variation in the power drawn during the process of machining. This is shown in figure 3.6. The power at each instant is divided into two parts – one for the initiation and propagation of cracks and the other for the build-up of strain energy in the stress field. The energy for the initiation and propagation of cracks can be obtained directly from the tool or from the strain energy built up during previous instants of the tool motion. Thus there is a continuously changing energy flow at the tool workpiece interface.

## 3.5 Investigation of Surface Texture Formation

One of the ultimate objectives of machining ceramics is to achieve a high degree of geometric accuracy with a designed part. The texture formed on a machined surface plays a key role in this regard. Based on the previous discussion, the machined surface can be viewed as an assemblage of fracture surfaces left behind by chip formation. Therefore, unlike in materials cut in the ductile mode, there is no concept of the ideal surface generated by shear in the absence of vibrations. Correspondingly, the surface generated predominantly by fracture would be very different in quality from the surface generated by shearing the material. These differences can be investigated through a study of the surface and of the chips produced in the process of material removal.

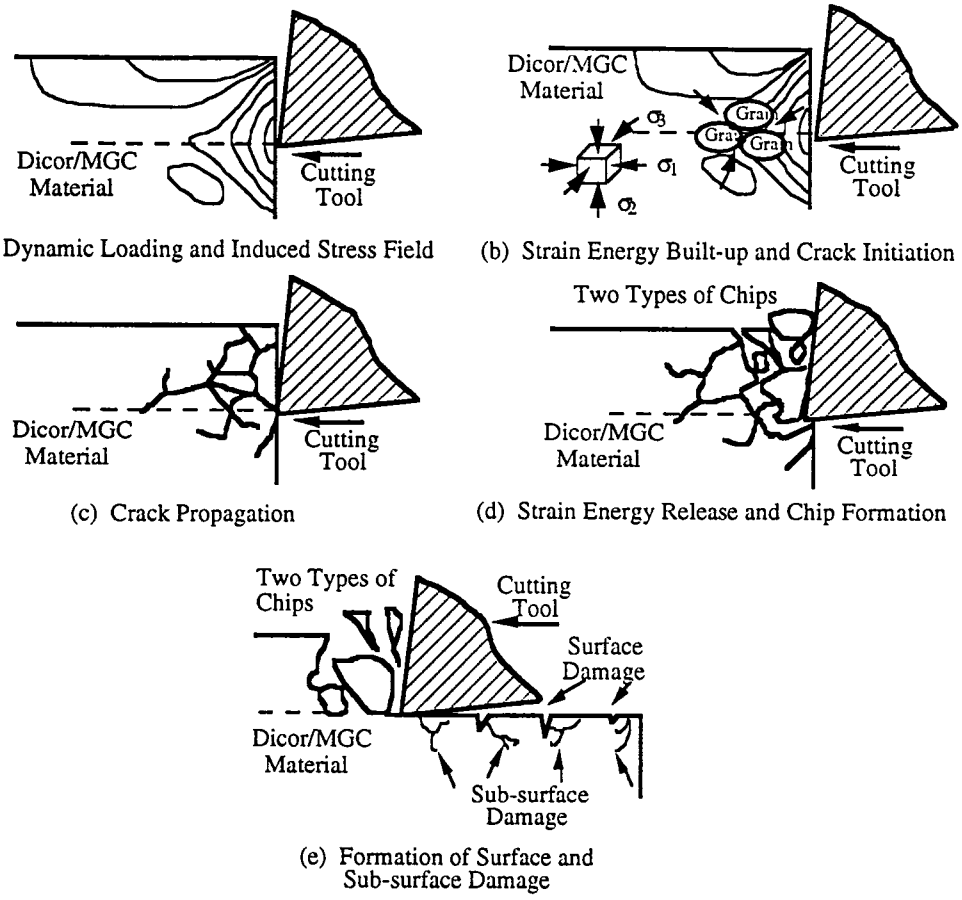


(a) Dynamic Loading and Induced Stress Field

(b) Strain Energy Built-up and Crack Initiation

(c) Crack Propagation

(d) Strain Energy Release and Chip Formation

(e) Formation of Surface and Sub-surface Damage

Figure 3.7: Model of Machining Mechanism

### 3.5.1 Volumetric Distribution of Chips

From the model proposed in section 3.4, it can be expected that the differences in cutting conditions and correspondingly in the stress distributions induced, would manifest in some form in the chips that are removed from the material. A state of high stress offers different conditions for crack nucleation and propagation than a less severely stressed state. To study the effect of cutting parameters on the chips formed, in this research, a systematic examination of the chip fragments is undertaken. It is expected that the distributions of chip sizes would be particularly instructive in the mechanisms of surface texture formation.

### 3.5.2 Quality of Machined Surface

The roughness of the machined surface is related to the chip formation process. Changes in the characteristics of chips formed would therefore manifest as a change in the surface roughness of the machined specimen. A study of the variation of surface roughness with cutting conditions would be informative regarding the surface formation process. Since a mechanical stylus is used for this measurement, the narrowest surface feature that can be studied is limited by the dimensions of the stylus tip. Hence, surface cracks cannot be studied using this method. Nevertheless, the surface roughness parameter is expected to bear out effects of the cutting conditions on the surface formation process.

## 3.6 Environmental Effects on the Machining Process

As mentioned in section 3.1, the environmental conditions present at the interface of the tool and workpiece, can be used to alter the loading conditions. This can be used as a method of controlling the stress distribution in the workpiece. This offers the possibility of the use of chemicals to perform crack controlled machining. Experiments performed on alumina have demonstrated this possibility[Hwa92]. Factors that could affect the efficiency of a chemically assisted machining process are,

- Interaction between the cutting fluid, tool and workpiece materials.
- Access to the cutting fluid at the high cutting speeds involved.
- Temperature of the cutting fluid that would maximize the rate of reaction.

A submerged machining process is proposed to study the effects of machining the specimen while submerged in a bath of the active chemicals at a controlled temperature. In a submerged state, increased access to the chemicals can be expected to increase the effects of chemical assistance to the machining process.

## 3.7 Summary

The discussion in this chapter served to lay a starting point for the understanding of the mechanics of material removal in ceramic materials and to lay guidelines to be followed in this study. The discussion can be summarized in the following manner.

- Material removal in ceramic machining is predominantly through brittle fracture. The stress distribution determines the distribution of stress concentration through the material and is therefore an important parameter in achieving microcrack-controlled machining.

- Machining of ceramic materials is characterized by a five-stage process, namely, dynamic loading, strain energy build-up and crack initiation, crack propagation, and chip formation.

- The environment during the machining process can be used to better control the tensile stress distribution and consequently the material removal process.

# Chapter 4

# Experimental Setup

This chapter presents a brief description of the apparatus used in this study. The design and fabrication of the equipment necessary for this study is reviewed in some detail.

## 4.1 Machine Setup

The experiments for this study were performed on the CNC Machining Center MATSUURA MC510V. This is a computer numerically controlled machine and capable of importing programs from an IBM PC. All equipment required was adapted to this machine. A photograph of the machine is shown in figure 4.1

## 4.2 Machining the Ceramic

The ceramic material used for this study was in the form of 6 inch long bars of rectangular cross-section. Since the machined specimens would have to be examined under the Environmental Scanning Electron Microscope, the maximum

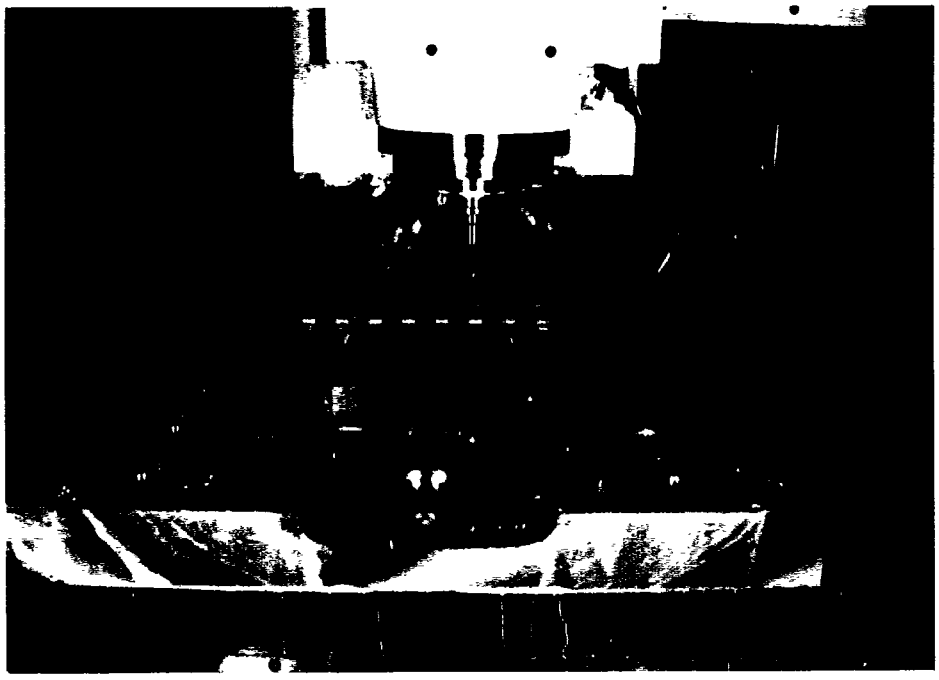

Figure 4.1: CNC Machining Center

dimension of each specimen was limited to 1 inch. For this reason, the bar was cut into smaller pieces with the help of a diamond saw. These bars did not have parallel or even flat sides in most cases. Furthermore, ceramic materials crack easily under concentrated loads. Hence, they could not be held in the vise directly. A fixture was designed for the purpose of holding the specimen during the machining process. One such fixture is shown in figure 4.2. A typical experiment was performed on a block with 8 or 16 such fixtures machined into it. Each ceramic specimen was glued to the fixture using epoxy adhesive. Once the test was complete, the fixturing block was cut up so that each ceramic sample could be placed in the ESEM.

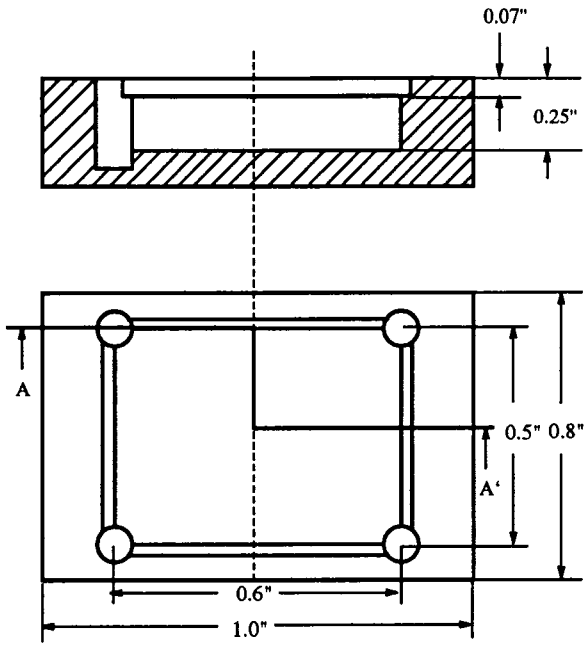


Figure 4.2: Fixture for Machining Ceramic

## 4.3 Chip Collection

In the case of ductile materials, since the material is capable of a fairly large amount of plastic flow, the chips formed from the shearing of the workpiece are much larger in size than the chips formed during the machining of brittle materials. In ceramic materials, since the chips are formed through brittle fracture, they can be smaller than $10\mu$m across. Hence filtration cannot be performed on line. Therefore, for the purpose of experimentation, the spent cutting fluid is collected and then filtered. When the filter paper is dried and tapped gently, the chips fall out separately.

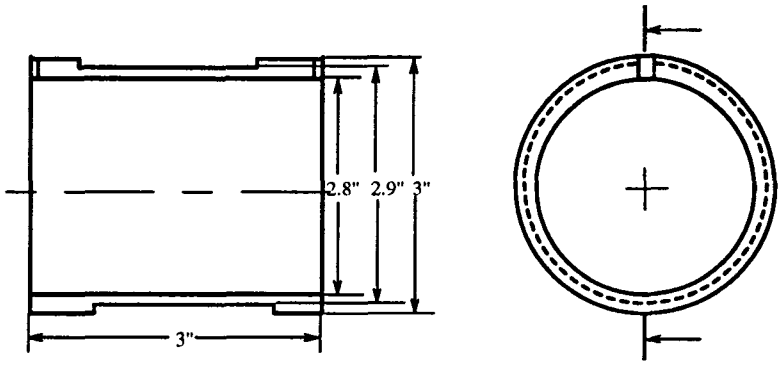


Figure 4.3: Mechanical Drawing of the Cylinder

## 4.4 Submerged Machining Apparatus

One part of this research involved testing the effects of cutting fluids on the cutting process. For this purpose, it was decided to conduct submerged machining where the workpiece is held submerged in the cutting fluid during the process of machining. In this study, the effect of temperature of cutting fluid on the cutting efficiency was also studied. To perform the test, a submerged machining apparatus was designed and fabricated. The design objectives of the apparatus were the following.

1. The workpiece must be machined when submerged in the cutting fluid.

2. The apparatus must be capable of measuring and recording forces in three directions and the torque applied by the tool on the workpiece.

3. The cutting fluid must be maintained at a constant temperature that can be set at the beginning of each experiment

This section deals with the details of the design and fabrication of this apparatus.

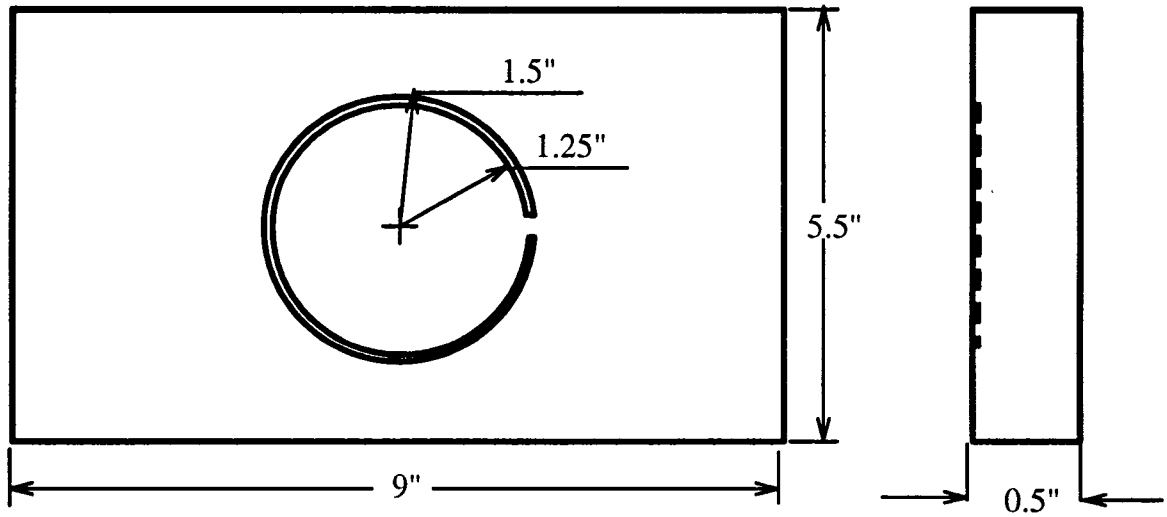


Figure 4.4: Mechanical Drawing of the Base Plate

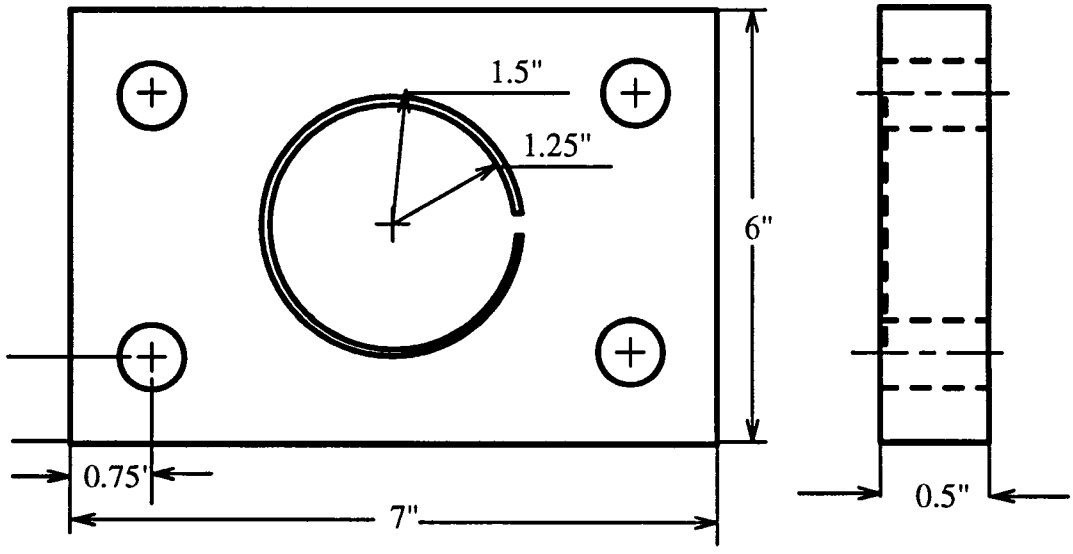


Figure 4.5: Mechanical Drawing of the Top Plate

### 4.4.1 Structural Design

The structural design of the apparatus is shown in figures 4.3, 4.4 and 4.5. The base plate is to be mounted into the vise on the CNC machine. Attached to the base plate is a cylinder which acts as the strain element. Strain gages are mounted on this surface to measure the strains produced by the loading on the cylinder. The top plate provides a surface to hold the tank of cutting fluid and the workpiece. The cylinder is made out of aluminum so as to increase its sensitivity to loads. Marking a trade off between the need for sufficient space to mount the strain gages and the need for low stiffness, the diameter and height were chosen to be 3". The cylinder has a thickness of 1/16". Since the forces to be measured are quite small, a small cylinder wall thickness was considered to be sufficient.

The top and base plates are made out of steel. The aluminum cylinder is attached to the two steel plates using 2–ton epoxy adhesive. A circular arc was milled into the plates so as to fix the orientation of the cylinder.

The vise blocks are made of aluminum and serve to restrain the workpiece during machining. These are mounted on the top plate through holes in the tank, thus holding the tank in position too. One of the blocks carries three set screws that can be tightened to hold the workpiece.

### 4.4.2 Temperature Control

In order to maintain the temperature of the fluid tank at a known value, the tank is equipped with a heater. A thermocouple junction serves as the sensor for feedback to the controller. The controller receives the signal from the thermocouple and controls the heater through on/off manipulations or by varying the

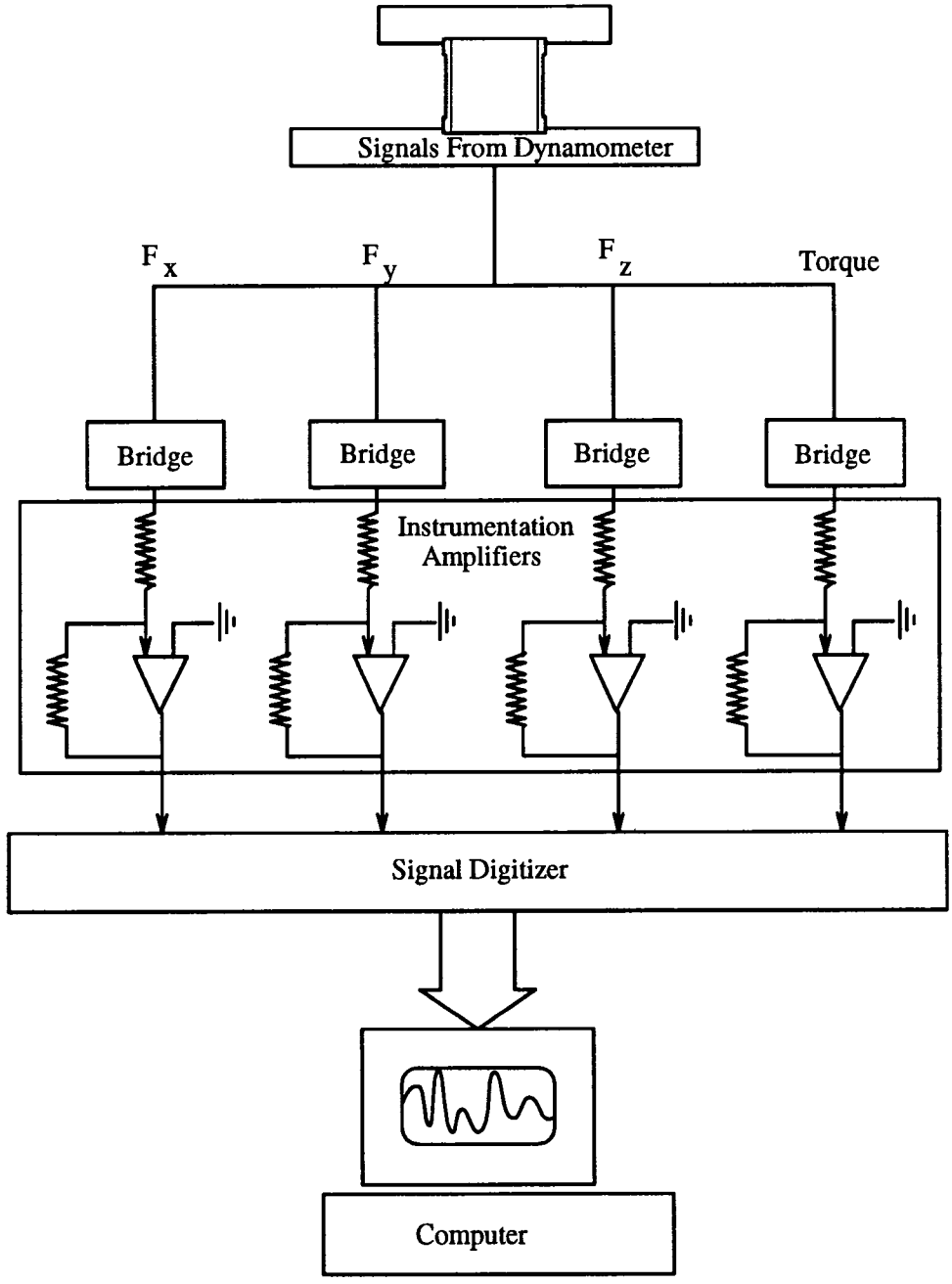


Figure 4.6: Schematic Representation of the Force Measurement System

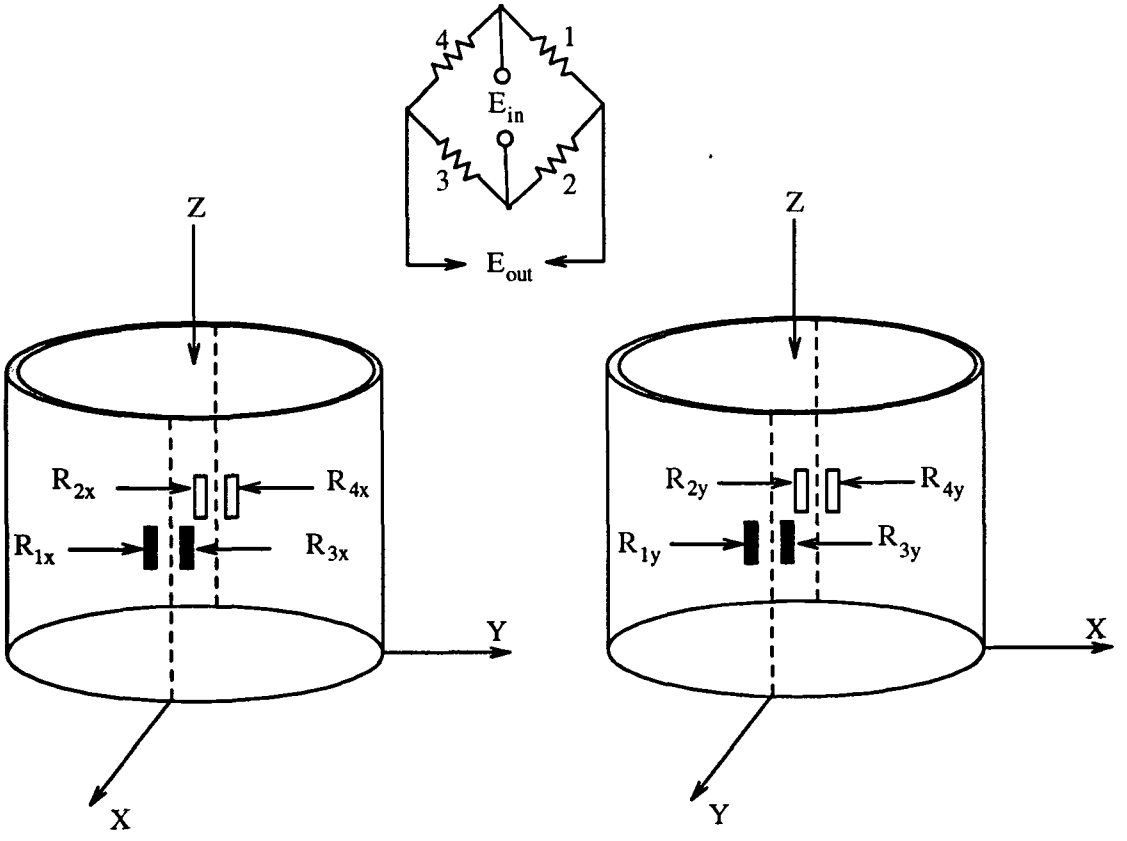


Figure 4.7: Strain Gage Orientation for Measuring $F_x$ and $F_y$

energy supplied to the heater. In this manner, every experiment was performed at a known temperature.

### 4.4.3 Force Measurement

The third design requirement was to be able to measure forces in three directions and the torque exerted by the tool on the workpiece. For this purpose, in the structural design, the apparatus was equipped with a strain element in the form of a cylinder. All the forces experienced by the workpiece are transmitted to the machine tool through this component. As a result, the cylinder undergoes deformation. Strain gages are used to measure these strains. The gages are connected in the form of bridges which convert the strain into electrical voltage signals. These signals are amplified using a voltage amplifier and recorded in a computer using a data acquisition system. The system is shown schematically in figure 4.6.

Initially, standard foil gages were used for this purpose. On conducting experiments, it was discovered that the sensitivity of the foil gages was insufficient to record the forces encountered. It was then decided to replace the foil gages by semiconducter strain gages. While foil gages have a gage factor of about 2, the semiconducter gages used have a gage factor of 155.

The configuration of strain gages in the four cases is shown in the figures 4.7 and 4.8. Since semiconducter gages are sensitive to temperature variations, it was necessary to use full Wheatstone's bridges.

The forces recorded by this method were transferred to the UNIX workstation and MATLAB was used to analyze the data.

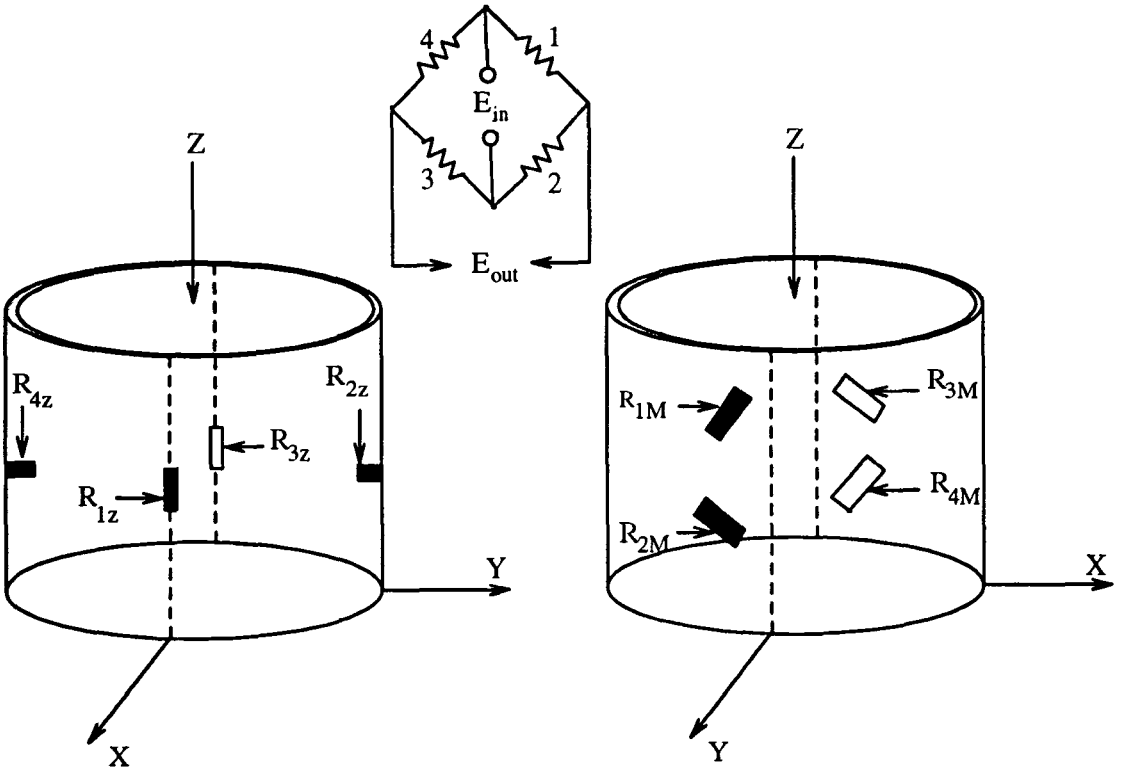


Figure 4.8: Strain Gage Orientation for Measuring $F_z$ and $M_z$

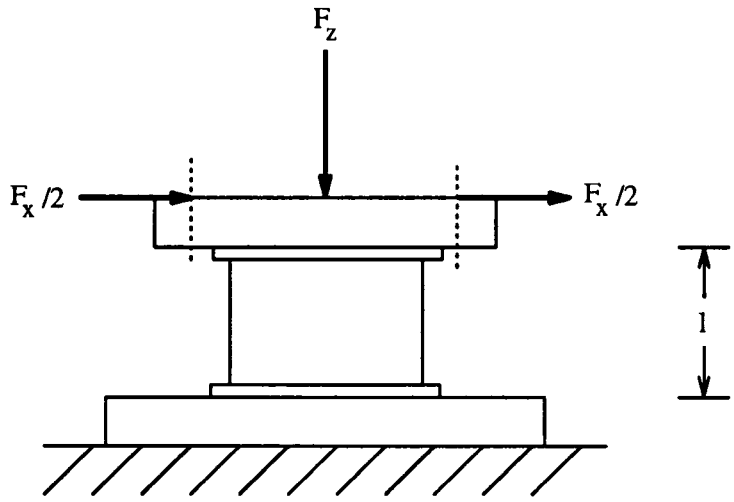


Figure 4.9: Two Forces on the Dynamometer

### 4.4.4 Force Data Analysis

The strain gages bonded to the aluminum cylinder measure the strains of the cylinder at that point and in one fixed direction. The following analysis is essential to derive the information about forces on the workpiece from these measured strains.

Figure 4.9 shows two forces acting in one plane on the workpiece. The vertical force is termed $F_z$ and the horizontal force, $F_x$. In this case, $x$ is the direction of the feed motion. But the analysis is similar for the case of $y$. For the case of $z$, the cylinder is a compressive member. Since the gage is placed in the thin portion of the cylinder, the force $F_z$ is given by the following expression.

$$F_z = \epsilon AE \tag{4.1}$$

In this equation, $A$ stands for the cross-sectional area and $E$ is the modulus of elasticity for aluminum. $\epsilon$ is the strain along the axis of the cylinder.

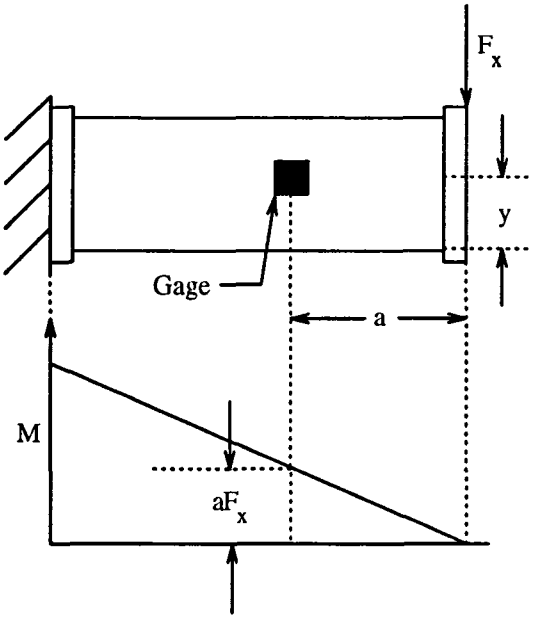


Figure 4.10: Moment Diagram for $F_x$ Loading

In the case of $F_x$, the force is obtained as a function of the moment applied about the base of the cylinder. Since the moment $M$ and more specifically, the value $\frac{M}{EI}$, where I stands for the area moment of the cross-section, varies through the length of the cylinder, the position of placement of the gages along the length plays an important role. This variation is shown in figure 4.10. Using the nomenclature shown in the figure, the force $F_x$ can be derived in the following manner.

$$\frac{M}{I} = \frac{\sigma}{y} \tag{4.2}$$

$$M = aF_x \tag{4.3}$$

$$\frac{F_x a y}{I} = \epsilon E \tag{4.4}$$

$$F_x = \frac{\epsilon E I}{a y} \tag{4.5}$$

In equations 4.2 to 4.5, all the properties have been considered at the cross-

section where the gages have been bonded. The meanings of the variables can be seen in figure 4.10.

## 4.5 Environmental Scanning Electron Microscope

One of the main tools used in this research to study the machined surface and the chips produced is the ESEM. The disadvantage of using conventional SEM is that the specimen to be studied has to be conducting. Hence to use the machine to study ceramic specimens, they have to be covered with a thin conducting layer of carbon first and this hides some aspects of the surface that may give valuable information. But with an Environmental SEM, it is possible to study non-conducting specimens without covering them with conducting layers. This preserves the surface in the original condition. It is also possible to perform Energy Dispersive Studies (EDS) on the specimen in order to find out the chemical composition of the surface layer. This is an extremely useful tool in the study of the effects of various cutting fluids on the machining process.

The ESEM functions using an electron beam as the source. On interacting with the specimen, the reflected beams carry the required information. A detector is used to collect these beams and convert the information into a visual form which is viewed on a CRT terminal. In the case of EDS, X-rays are bombarded on the specimen and the resulting radiation gives the dispersion spectrum of the specimen. This is a characteristic of the elements that form the specimen and with the aid of relevant software, it is possible to arrive at the exact elements that have that particular dispersion spectrum.

## 4.6 Surface Roughness Measurement

The surface roughness was measured using a stylus type profilometer. This consists of a stylus with a very small tip radius. The stylus is traced over the surface at a controlled speed and the displacement of the stylus tip is measured. This signal is transformed to eliminate low frequency variations that are assumed to be waviness and deviations in component geometry. From the transformed signal, the $R_a$ value is obtained from the expression in equation 4.6. In this equation $L$ refers to the trace length, and $y(x)$ is the profile as a function of the horizontal coordinate $x$.

$$R_a = \frac{1}{L}\int_0^L |y(x)|dx \tag{4.6}$$

This quantifies the roughness of the surface for comparison.

# Chapter 5

# Experimental Study of Ceramic Machining

This chapter summarizes the experimental work performed to gain an understanding of the mechanisms of material removal and the effect of the environment on the machining performance. The work previously accomplished at the Advanced Design and Manufacturing Laboratory is also reviewed for the purpose of comparison.

## 5.1 Current Status

Research has been conducted in the Advanced Design and Manufacturing Laboratory in an effort to understand the basic mechanisms involved in the machining of ceramic materials [Hwa92, Bea90]. Alumina was the material selected for this study. Turning alumina bars under different cutting conditions formed the basis of the experiments. During these experiments, the cutting forces in two directions were measured using an instrumented tool holder. The forces were used to

obtain estimates of the friction factor under different machining conditions. It was reported that addition of a chemical resulted in a significant change in the friction factor, while the net force remained approximately the same. The forces measured were used to compute the unit cutting force which is defined as the cutting force per unit cutting area of the material. It was observed to be significantly higher than the values predicted for conventional ductile materials such as metals. Based on these observations, an empirical formula for the variation of unit cutting force for brittle materials was suggested.

Scanning Electron Micrographs of the chip fragments collected during machining were taken. It was observed that some chip fragments showed evidence of plastic flow. From the predominance of chip fragments formed by brittle fracture, it was suggested that the machining mechanism involves a small amount of plastic flow coupled with brittle fracture as the significant mechanism of material removal. A preliminary model of material removal during ceramic machining was proposed.

The effect of a chemical additive on the unit cutting force and the friction factor was explained by the possible formation of compounds at the interface of the tool and workpiece material. But this was not substantiated in any manner. This research seeks to build on the experimental evidence obtained so far and study some of the issues more deeply.

## 5.2 Methodology of Investigation

This section summarizes the methodology adopted to study some issues involved in ceramic machining. A brief review of the experimental procedures used is also

included.

### 5.2.1 Selection of Ceramic Material

As stated in section 5.1, alumina was the primary test material in the previous study. For the purpose of this study, Dicor/MGC material was chosen as the test ceramic. Dicor/MGC belongs to the class of tetrasilicic mica glass ceramic materials. This material is produced from glasses based on the quaternary system $K_2O - MgF_2 - MgO - SiO_2$ with additions of $Al_2O_3$ and $ZrO_2$[D91]. This material has a unique microstructure consisting of mica flakes of approximately 70 percent by volume dispersed in a non-porous glass matrix. It has been used for dental restorations as its physical properties such as hardness, density, thermal conductivity and translucency closely match those of human enamel. The cleavage or splitting along the planes of mica flakes, is aided by stress concentration at the interface between the mica flakes and the ceramic material. This situation is similar to the stress concentration around inclusions present in free-machining steels, providing a mechanism for its machinability.

In contrast to Dicor/MGC, the alumina used as the test material for previous experimentation was $99.8\% Al_2O_3$. As a result of this basic difference in microstructure, Dicor/MGC can be expected to respond differently to the machining process.

### 5.2.2 Selection of Tool Material

It is well known that the material properties of the cutting tool and workpiece determine the type of tool that can be used. Of these material properties, the hardness is the most important consideration. It is often recommended that the

tool be at least 5 to 6 times as hard as the workpiece material[ZSK94]. The hardness of Dicor/MGC is about $3.4GPa$. Two types of tools were selected for the experiments. These are cemented tungsten carbide and high speed steel tools. The hardness of these tool materials are $22GPa$ and $18GPa$ respectively, and are at least 5 times as hard as the ceramic material.

### 5.2.3 Preliminary Scratch Test

Since Dicor/MGC is a relatively new ceramic, knowledge about the machinability and the difference between Dicor/MGC and other ceramic materials is limited. A preliminary scratch test was designed to study the basic mechanism of material removal. This experiment involved the use of a diamond indenter to scratch the surface of a Dicor/MGC specimen. The experiments were performed under different conditions of environment (lubrication) and depth of cut. The varying depth of cut was simulated by holding the specimen at an inclination of $1.15^{o}$. This caused the indenter to cut deeper as it progressed along the scratch. The experimental setup used is shown in figure 5.1.

As the scratch was being made, forces in two directions were measured. The ratio of these two forces gives an estimate of the coefficient of friction. The scratches were also observed under the ESEM to study the effects of the environmental conditions.

### 5.2.4 First Set of Experiments

After the scratch tests on Dicor/MGC, it was decided to conduct experiments in the actual machining environment. This set of experiments was designed to fulfill the following objectives.

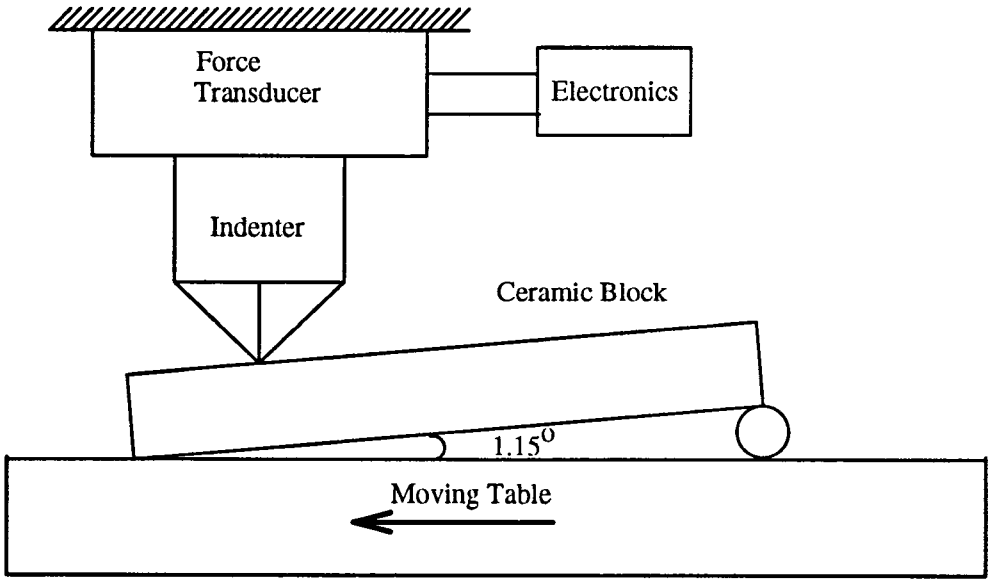


Figure 5.1: Experimental Setup for the Scratch Test

- With limited knowledge of the behavior of the material in the machining process, it was necessary to get an idea of the settings for cutting parameters that would be suitable for this material.

- Since this is a machinable ceramic, HSS and carbide tools were used to machine it. It was necessary to observe the response of the ceramic to different tool materials.

- Though the scratch test demonstrated the effect of lubrication on the material removal mechanism, it was necessary to test this in the real machining environment where access of lubricant to the cutting zone is limited and cutting speeds can be quite high.

It was decided to perform a five factor full factorial design resulting in $2^5$ experiments. The five factors used were feed, speed, depth of cut, type of tool and presence of cutting fluid. The range of variables used is shown in the table

| parameter | Low | High | Units |
|---|---|---|---|
| Feed | 0.2 | 0.4 | $\frac{in}{min}$ |
| Depth of Cut | 0.0029 | 0.006 | $in$ |
| Spindle Speed | 400 | 600 | $rpm$ |
| Coolant | On | Off | - |
| Tool | HSS | CC | - |

Table 5.1: Range of Variables Used in the $2^5$ Experiments

5.1. The fluid used for this purpose was a commercially available emulsifiable oil. The details of this chemical are listed in appendix A.

The following procedure was followed in performing the 32 experiments. To reduce variation in depth of cut, introduced by human error, 16 specimens were mounted on a single sheet of plexiglass. For this purpose, the fixture slots described in figure 4.2 were milled into the plexiglass. The specimens were then glued into the fixtures with the aid of an epoxy resin adhesive. Two experiments were conducted on each specimen. For the entire experiment, three end milling tools were used. The specimens were first prepared using a HSS tool. This involved machining each specimen to ensure flatness and same height as the other specimens. Once this was accomplished, the surface of the specimens was set to be a depth of cut of zero and the other two tools were used to perform the experiments. One of the tools used was a HSS tool and the other was a carbide tool. In order to eliminate a significant difference in the height setting of the two tools, the procedure for setting the tool lengths was repeated five times for each tool. Having ensured that the procedure is sufficiently repeatable, one of the tool settings was used for the experiment. Compressed air was used to clear

away the chip fragments during machining without cutting fluid. This helped minimize undesirable effects like abrasion between the chips and the workpiece.

### 5.2.5 Second Set of Experiments

After the first set of experiments, a second set of experiments was performed with the following objectives:

- The variation of surface roughness with the cutting parameters observed in the first set of experiments showed some interesting results and it was desirable to corroborate these results through further experimentation.

- It was necessary to study the chips that are produced during the machining process for clues to the material removal mechanism.

The experimental conditions for the second set of experiments were determined from the following considerations:

- It was observed that the tools used for the first set of experiments showed no signs of wear after the 32 experiments. This can be seen from the SEM micrographs in figure 5.2. This suggested that the material removal rate could be increased.

- For the purpose of studying the chips produced during the machining process, the chips would have to be greater than a certain size to make filtration possible. The cutting conditions in the first set of experiments produced chips that were sufficiently small to cause a large fraction of chip fragments to escape filtration.

| parameter | Low | High | Units |
|---|---|---|---|
| Feed | 0.2 | 0.4 | $\frac{in}{min}$ |
| Depth of Cut | 0.014 | 0.028 | $in$ |
| Spindle Speed | 400 | 600 | $rpm$ |

Table 5.2: Cutting Parameters for Second Set of Experiments

- Analysis of the results obtained in the first set of experiments showed that the tool material did not have a significant effect on the machining process. The cemented carbide cutting tool was chosen for experimentation.

The design of experimentation is shown in figure 5.3. The values shown in parentheses are the surface roughness values ($R_a$) in $\mu m$, for the different machining conditions. This set of experiments is designed primarily to study the effect of the cutting parameters on the machining efficiency and the cutting mechanisms involved.

One of the important inputs to the study of cutting mechanisms is the chip fragments formed during the machining process. The chip fragments were collected from a preliminary experiment performed in air without the application of coolant. These were observed under the ESEM and the smallest chip was measured to be approximately $10\mu m$ across. A typical SEM micrograph of the chip fragments collected is shown in figure 5.12. With this information, it was decided to perform off line filtration of the spent cutting fluid since the time for filtration was sufficiently high to make on-line filtration infeasible. Two stages of filtration were used. The first was to filter all particles with a minimum dimension greater than $25\mu m$. The second stage filtered particles with a minimum dimension greater than $7\mu m$. Chip fragments from different machining condi-

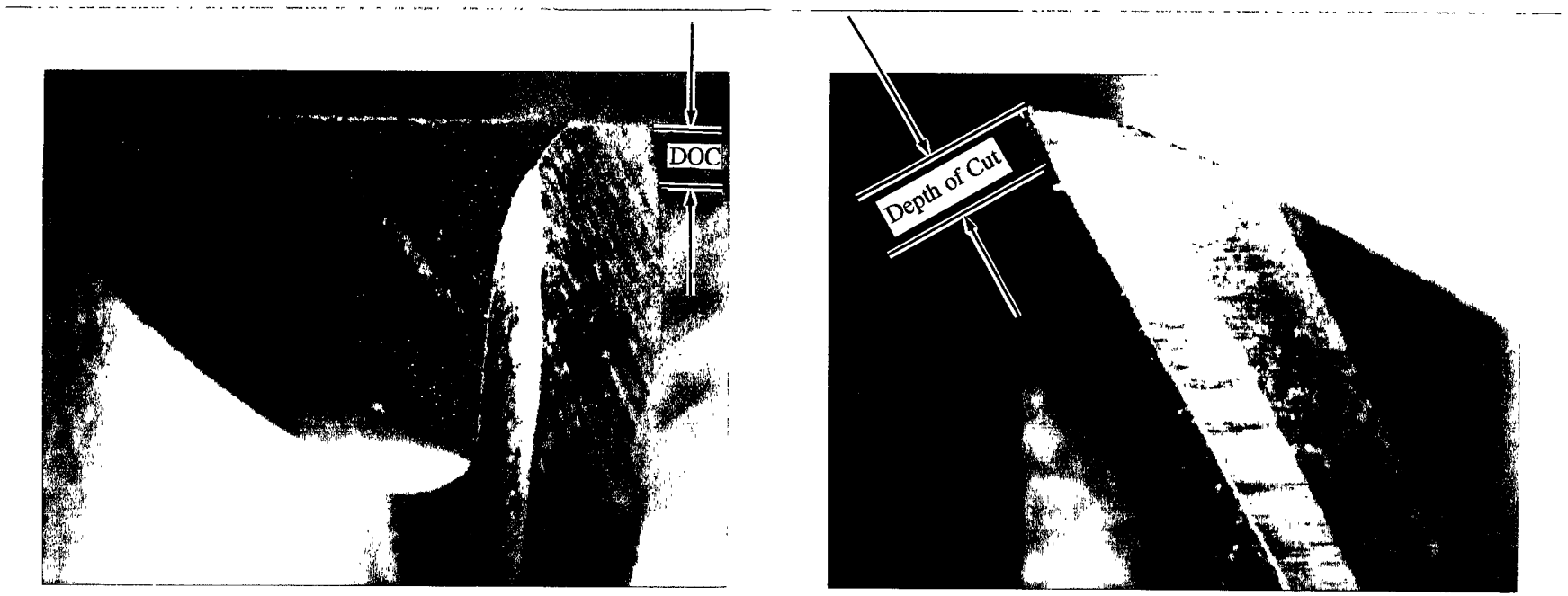


Figure 5.2: Tool Wear After First Set of Experiments

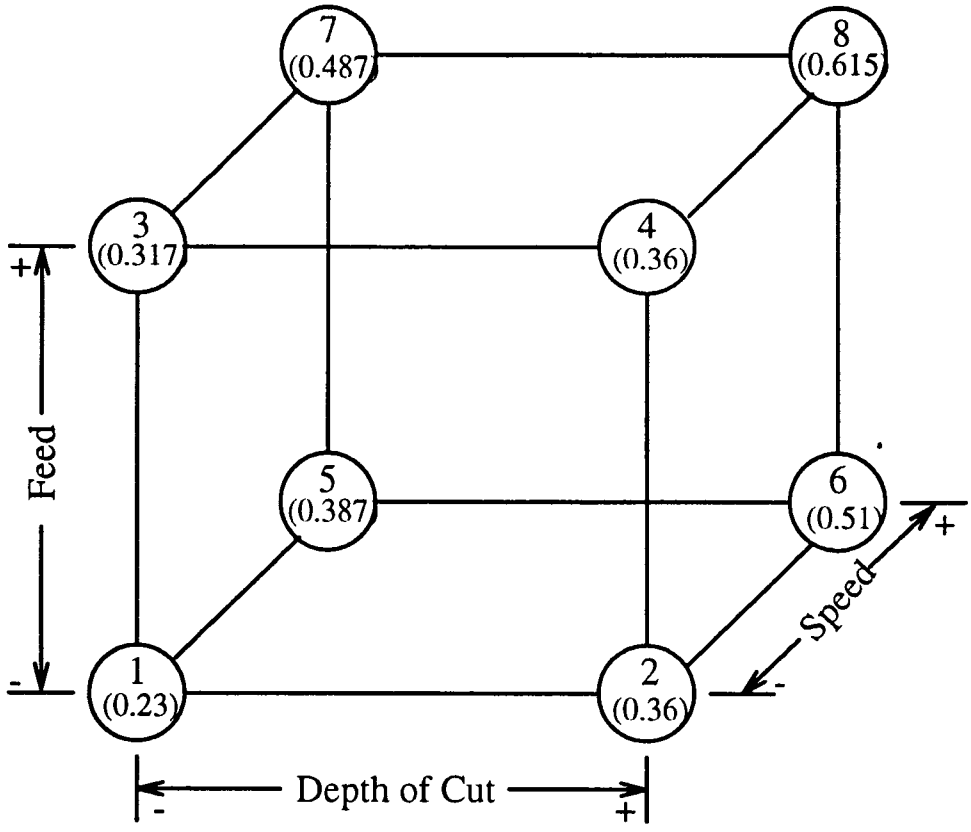


Figure 5.3: Design of Experimentation for Experiment Set 2

tions were collected in different boxes and transferred to standard SEM stubs for observation under the ESEM. Double sided adhesive tape was used to hold the chip fragments on the stubs.

The surface roughnesses of the specimens machined in this set of experiments were also obtained using the profilometer. These were used in correlation with the chip fragments collected in order to obtain an insight into the material removal process.

### 5.2.6 Submerged Machining

Submerged machining constituted the third and final set of experiments. The objectives of these experiments were the following:

- It was desirable to measure the cutting forces encountered by the cutting tool, to gain an insight into the mechanisms involved.
- Since the cutting speeds are quite high in machining processes, there is a problem of access of cutting fluid to the cutting areas. To study the efficiency of cutting fluids, submerged machining was designed as a means of possibly increasing access of cutting fluid to the cutting regions. This would aid in an investigation of the chemo-mechanical effects of the environment on the machining performance.
- The effect of temperature of the cutting fluid on the machining process could be studied.

The experiments performed in this set were designed with the above considerations. The experimental conditions described in table 5.2 were repeated

three times with different environmental conditions. The three cases considered were:

- Dry cutting with the use of compressed air to clear away chips.
- Submerged machining with the cutting fluid maintained at $65^{o}F$.
- Submerged machining with the cutting fluid maintained at $150^{o}F$.

## 5.3 Analysis of Specimens

This section deals with the types of analyses performed during and after the experimentation, on the machined specimens. The results of these tests are presented in this section.

### 5.3.1 Measurement of Forces

The results from the scratch tests are shown in figures 5.4 and 5.5. The two plots in each figure are for two trials of the scratch under the same experimental conditions. $F_z$ and $F_x$ are shown for each trial, where $F_z$ is the vertical force and $F_x$ is the horizontal force. The coefficient of friction can be calculated from these figures to be around 0.2 for the lubricated case and 0.5 for the dry case.

The third set of experiments were performed on the apparatus described in section 4.4. Forces were measured and are shown in figures 5.6, 5.7 and 5.8. In these figures, "cold" refers to $65^{o}F$ and "hot" refers to $150^{o}F$. The three numbers listed for each experimental condition are $F_z$ and $F_x$ in *Newtons* and the resultant force in the $xz$–plane. In this figure, $x$ refers to the direction of feed and $z$ refers to the axis of the spindle.

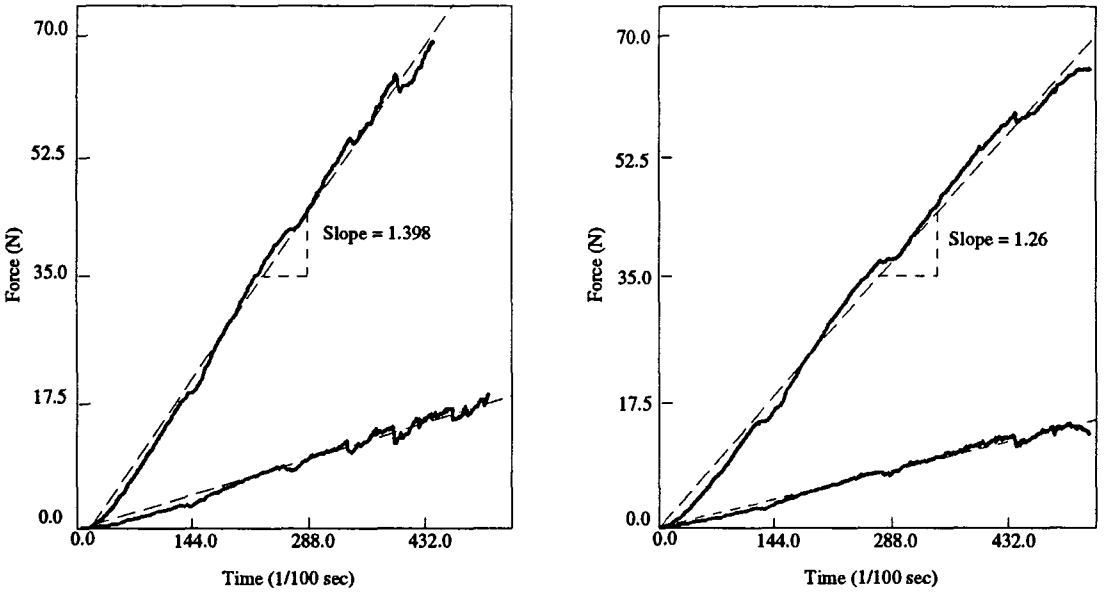


Figure 5.4: Forces Measured for Dry Tests

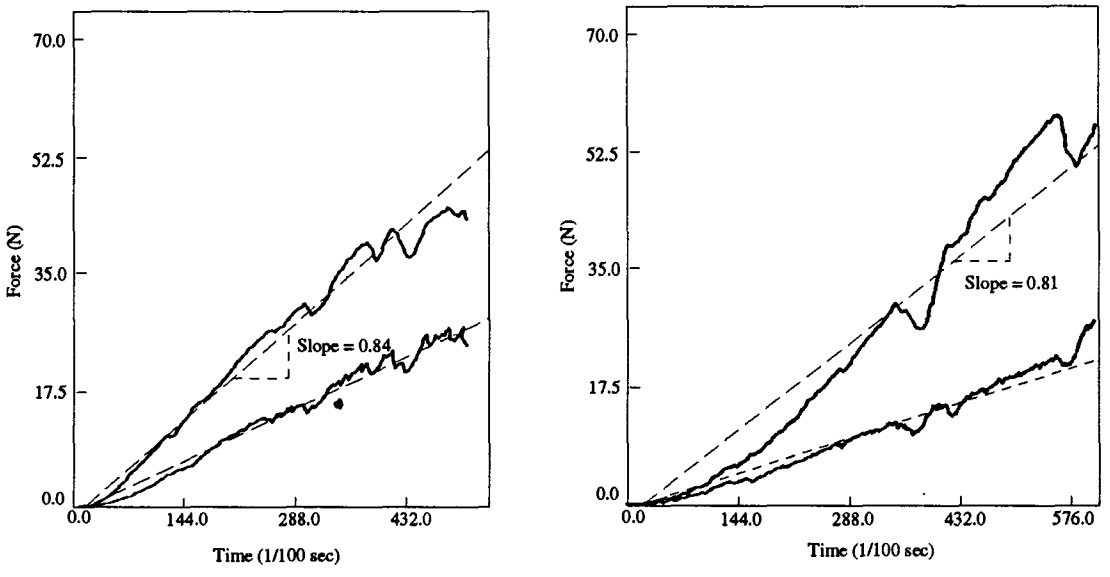


Figure 5.5: Forces Measured for Lubricated Tests

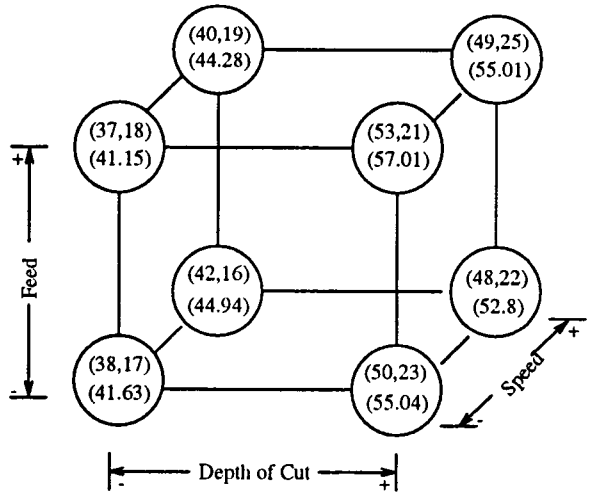


Figure 5.6: Forces in Dry Machining

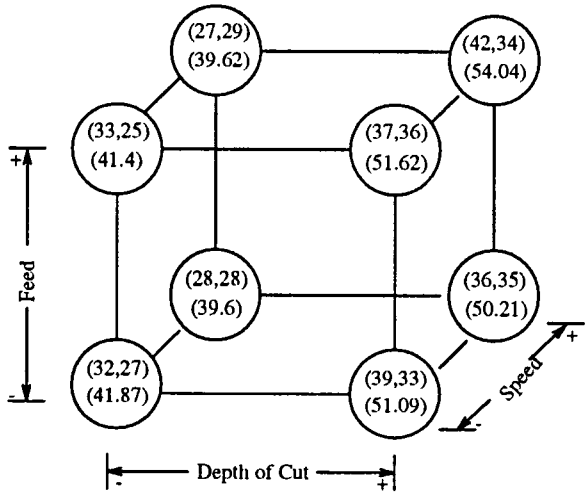


Figure 5.7: Forces in Cold Submerged Machining

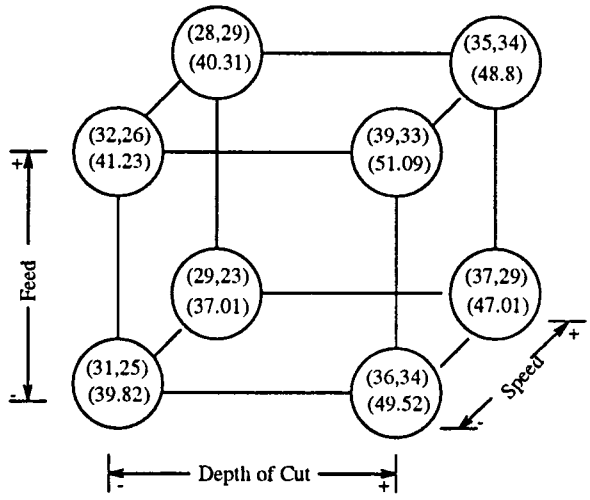


Figure 5.8: Forces in Hot Submerged Machining

### 5.3.2 Chemical Analysis

In the previous experiments with alumina, it was observed that there is a significant effect of the environment on the machining process. It was hypothesised that the interaction between the chemical and the workpiece material at the elevated cutting temperatures was responsible for the difference in friction factor encountered. To study further, the effect of chemicals on the machining process, chemical analysis of the machined surface was undertaken. Sixteen experiments in the first set of experiments were performed with the application of a commercially available cutting fluid while sixteen experiments were performed in air. These specimens were used for the chemical analysis. The ESEM coupled with an X-ray emitter was used for this purpose. A data acquisition system was used to collect the data and analyze it. The resulting spectrum is a superposition of the characteristic spectra of the constituent elements. A software program was used to decouple the individual components of the spectrum and compute the strength of each spectrum. The percentage composition of each element in

the test volume thus obtained was normalized against the element zirconium which is not present in the cutting fluid used for this experiment. The elements chlorine and oxygen were found to change significantly in the presence of cutting fluid during the machining process. The variation of their percentages are shown in figures 5.9 and 5.10. In these figures, the numbers shown are the percentage chlorine and the percentage oxygen in the surface layers, respectively. The empirical models derived from these results are shown in equations 5.1 and 5.2.

$$\begin{aligned} \%Cl &= 3.57 - 0.785(coolant) + 0.15(speed) + 0.14(feed) \\ &\quad +0.16(feed * DOC) \qquad (5.1) \\ \%O &= 3.03 + 0.29(coolant) + 0.17(speed) - 0.24(coolant * DOC) \qquad (5.2) \end{aligned}$$

The variation under different cutting conditions and environmental conditions can be observed. This substantiates the effect of a chemical additive on the surface during the machining process. It is assumed here that since the ceramic material is very inert at room temperatures, chemical interactions studied here occur predominantly at the elevated temperatures present at the tool-workpiece interface during the process of machining. For example, the temperature at the tool–work interface was observed to be between $700-800°C$ at the feed of $10\frac{mm}{min}$, depth of cut of $0.1mm$ and a cutting speed of $40\frac{m}{min}$[Hwa92]. The surface was therefore cleaned after machining, before chemical analysis was undertaken. In this manner, residual cutting fluid on the surface of the specimen did not corrupt the observations.

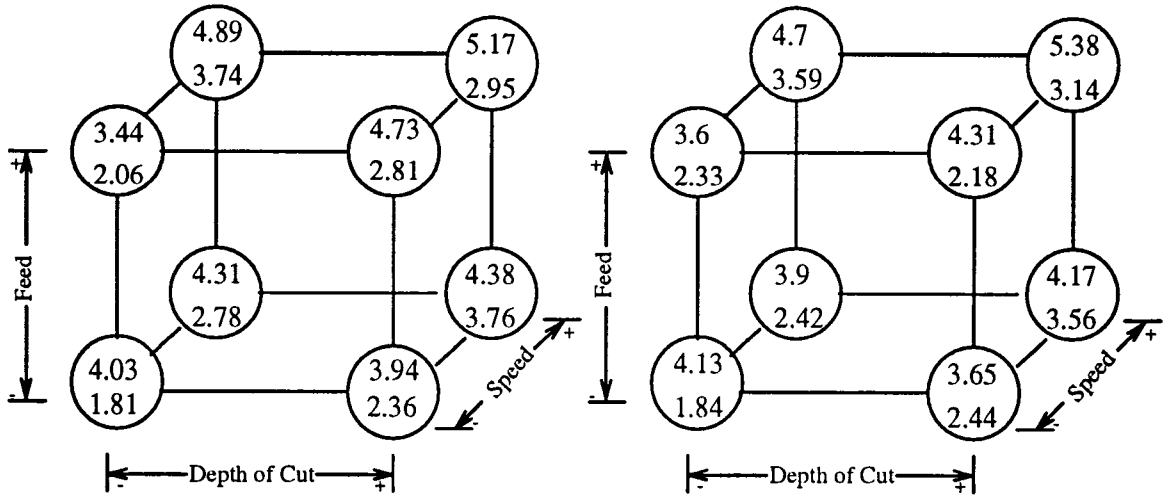


(a) HSS Tool (b) CC Tool

Figure 5.9: Chlorine and Oxygen Under Lubricated Cutting Conditions

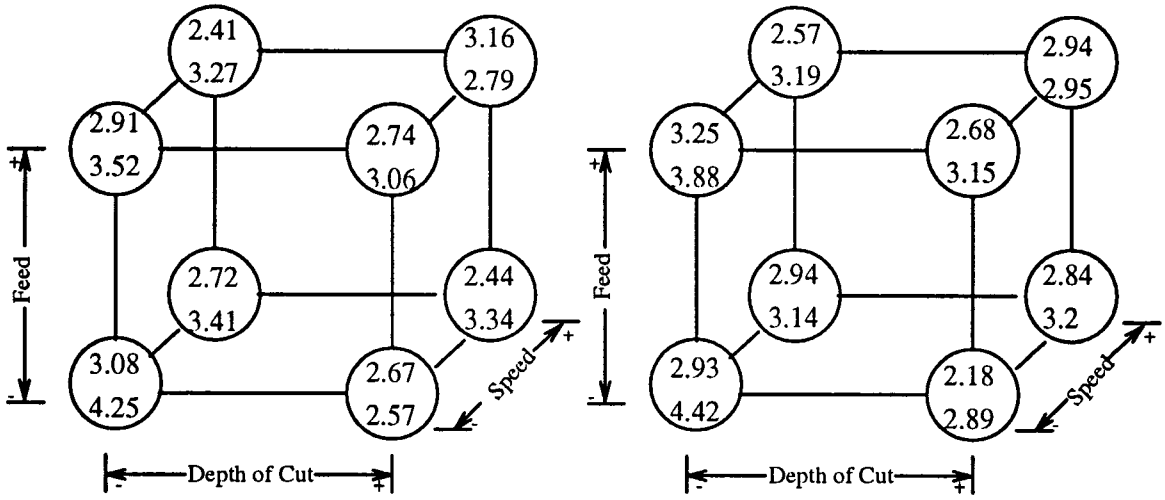


(a) HSS Tool (b) CC Tool

Figure 5.10: Chlorine and Oxygen Under Dry Cutting Conditions

| Exp. No. | Speed | DOC | Feed | Coolant | | Ratio |
|---|---|---|---|---|---|---|
| | $(rpm)$ | $(in)$ | $\frac{in}{min}$ | On | Off | $\frac{Off}{On}$ |
| 1 | 400 | 0.0029 | 0.2 | 0.195 | 0.275 | 1.41 |
| 2 | 400 | 0.0029 | 0.4 | 0.244 | 0.322 | 1.32 |
| 3 | 400 | 0.006 | 0.2 | 0.26 | 0.301 | 1.158 |
| 4 | 400 | 0.006 | 0.4 | 0.205 | 0.291 | 1.42 |
| 5 | 600 | 0.0029 | 0.2 | 0.261 | 0.341 | 1.31 |
| 6 | 600 | 0.0029 | 0.4 | 0.32 | 0.375 | 1.17 |
| 7 | 600 | 0.006 | 0.2 | 0.311 | 0.389 | 1.25 |
| 8 | 600 | 0.006 | 0.4 | 0.267 | 0.345 | 1.29 |

Table 5.3: Surface Roughness Values of First Set of Experiments

### 5.3.3 Analysis of Surface Quality

In addition to the chemical composition of the surface layer, the surface finish was also measured. As shown in figure 5.11, at different sections of the machined surface, the conditions of cutting vary due to the change in the direction of the motion of the cutting edge and the varying width of cut. In the figure, two representative points on the cutting trajectory are shown. The two points experience different cutting conditions. This may cause the surface roughness to be dependent on the position of the trace in a significant manner. For this reason, the roughness used was the average of the roughnesses obtained from three representative traces. The positions of these three traces are shown as a,b and c in figure 5.11.

The surface roughness values obtained from the 16 experiments performed with a cemented carbide cutting tool are tabulated in table 5.3. The empirical

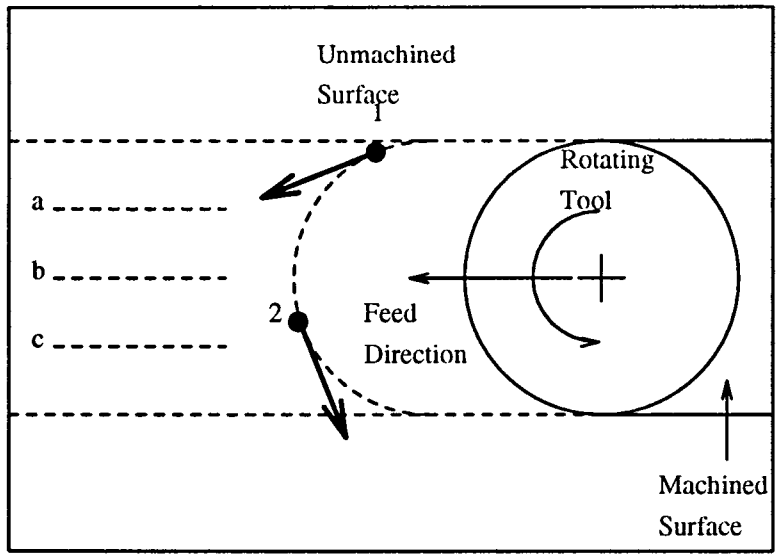


Figure 5.11: Top View of Progressing Cutting Tool

model derived from this data is listed in equation 5.3. The $R_a$ values for the second set of experiments are included in figure 5.3. The empirical model is shown in equation 5.4.

$$R_a = 0.293 + 0.035(coolant) + 0.028(speed) - 0.025(feed * DOC) \quad (5.3)$$

$$R_a = 0.407 + 0.092(speed) + 0.037(feed) + 0.052(DOC) \quad (5.4)$$

The surface roughness of the specimens machined in the third set of experiments is shown in table 5.4. In the table, dry refers to unlubricated cutting conditions, cold refers to submerged cutting at $65^oF$ and hot refers to submerged cutting at $150^oF$. The empirical models developed for this set of experiments are listed in equations 5.5, 5.6 and 5.7.

$$R_a(dry) = 1.753 + 0.203(feed) + 0.383(speed) \quad (5.5)$$

$$R_a(cold) = 0.26 + 0.088(feed) \quad (5.6)$$

$$R_a(hot) = 0.309 + 0.059(feed) \quad (5.7)$$

| Exp. No. | Speed $(rpm)$ | DOC $(in)$ | Feed $\frac{in}{min}$ | Dry $\mu m$ | Cold $\mu m$ | Hot $\mu m$ |
|---|---|---|---|---|---|---|
| 1 | 400 | 0.014 | 0.2 | 1.1 | 0.14 | 0.23 |
| 2 | 400 | 0.014 | 0.4 | 1.5 | 0.37 | 0.4 |
| 3 | 400 | 0.028 | 0.2 | 1.27 | 0.18 | 0.25 |
| 4 | 400 | 0.028 | 0.4 | 1.61 | 0.35 | 0.375 |
| 5 | 600 | 0.014 | 0.2 | 1.8 | 0.16 | 0.26 |
| 6 | 600 | 0.014 | 0.4 | 2.21 | 0.32 | 0.31 |
| 7 | 600 | 0.028 | 0.2 | 2.03 | 0.21 | 0.26 |
| 8 | 600 | 0.028 | 0.4 | 2.5 | 0.35 | 0.385 |

Table 5.4: Surface Roughness Values of Third Set of Experiments

### 5.3.4 Analysis of the Machined Chips

The chip fragments collected were photographed using the ESEM. The photographs were used to get an estimate of the chip size in each case. A square grid was used to measure out the area occupied by each chip enclosed within a fixed region in the photograph. This is shown in figure 5.12. This provided an estimate of the size of the chip. The mean and variance of chip size were determined for each cutting condition. These are tabulated in table 5.5.

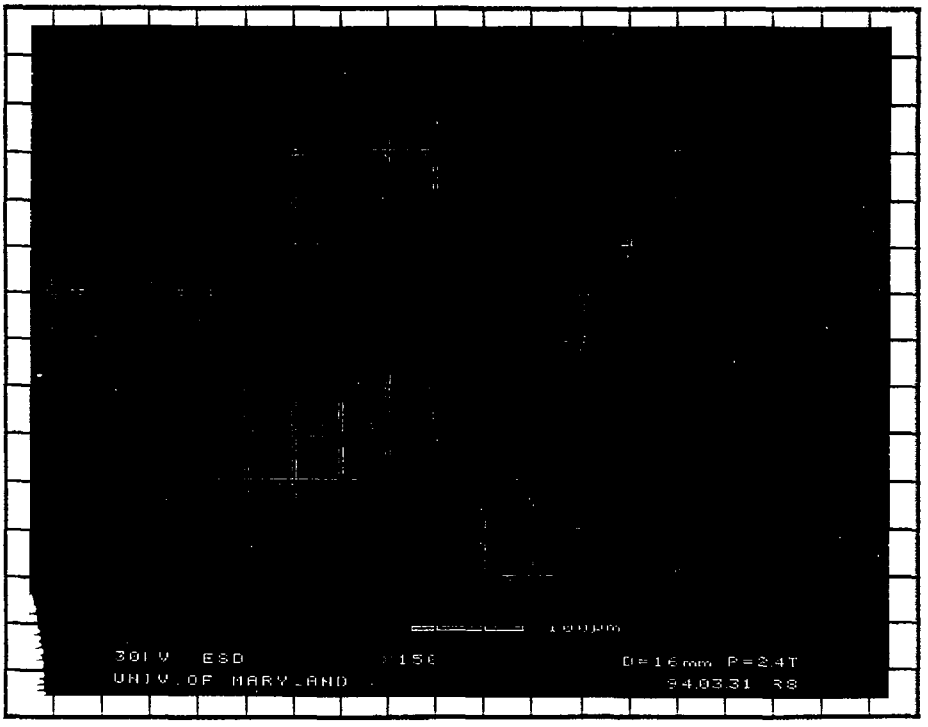


Figure 5.12: Grid for Chip Size Estimation

| Exp. No. | Speed $rpm$ | Feed $\frac{in}{min}$ | DOC $in$ | Average $\mu m^2$ | Variance $\mu m^4$ |
|---|---|---|---|---|---|
| 1 | 400 | 0.2 | 0.014 | 11.12 | 4.32 |
| 2 | 400 | 0.2 | 0.028 | 13.36 | 22.3 |
| 3 | 400 | 0.4 | 0.014 | 26.28 | 14.8 |
| 4 | 400 | 0.4 | 0.028 | 23.53 | 17.1 |
| 5 | 600 | 0.2 | 0.014 | 8.64 | 22.1 |
| 6 | 600 | 0.2 | 0.028 | 10.52 | 44.5 |
| 7 | 600 | 0.4 | 0.014 | 20.11 | 36.3 |
| 8 | 600 | 0.4 | 0.028 | 25.82 | 52.25 |

Table 5.5: Distribution of Chip Sizes

## 5.4 Summary

In this chapter, the experimental work done as part of this research has been outlined and the results from these experiments have been presented. In the next chapter, this information is used to gain insight into the material removal mechanisms and the effect of the environment on the machining performance.

# Chapter 6

# Discussions of Results

## 6.1 Mechanics of Material Removal

In this section, an attempt is made to understand the results of experimentation presented in chapter 5. The discussions in chapter 3 are used to interpret these results.

### 6.1.1 Effect of Cutting Speed

In the machining of conventional materials, experiments show a decrease in the cutting force with an increase in the cutting speed. This has been explained as the result of the softening of the material due to a rise in temperature at high cutting speeds. In the research performed on alumina in this laboratory, it had been observed that cutting forces occurring during the turning of alumina bars remain unchanged with an increase in cutting speed from $23.9\frac{m}{min}$ to $35.8\frac{m}{min}$ [Hwa92]. In this study on Dicor/MGC too, the cutting forces measured during milling have been observed to remain unchanged with an increase in the cutting

speed from $6.0\frac{m}{min}$ to $9.0\frac{m}{min}$. Based on these observations, a model for the effect of cutting speed on the material removal process is suggested in this section.

Typically, all materials show a drop in the yield strength with a rise in temperature. In the machining of conventional materials like metals, the unit cutting force experienced has been observed to be close to the yield strength at the temperature of the cutting zone[Sha84]. Ceramic materials differ from conventional materials in that the unit cutting force encountered in the machining of these materials is substantially lower than the ultimate tensile strength of the material. This can be seen from table 6.1. The unit cutting force in these cases is determined not by the tensile strength but by the fracture toughness of the material at the conditions existing in the vicinity of the cutting zone. The occurrence of brittle fracture as an important mechanism of material removal further supports this observation [Hwa92]. It is therefore important to consider the conditions present at the cutting zone during the process of machining and the effect on the fracture toughness of the material.

As the cutting tool progresses through the material, there are two conditions that change substantially with the cutting speed. These are:

- Temperature at the cutting zone
- Loading rate at the cutting zone

The loading rate, or strain rate, $\dot{\epsilon}$, is defined at each point in the material as the rate at which the material is getting deformed. With an increase in cutting speed, it is obvious that there is a corresponding increase in the loading rate in the cutting zone. The variation of fracture toughness of a typical brittle material with the loading rate is illustrated in figure 6.1. As can be seen, there is a decrease in the fracture toughness with the loading rate.

| Exp. No. | Speed $(rpm)$ | DOC $(in)$ | Feed $\frac{in}{min}$ | Dry $(GPa)$ | Cold $(GPa)$ | Hot $(GPa)$ |
|---|---|---|---|---|---|---|
| 1 | 400 | 0.014 | 0.2 | 18.42 | 18.52 | 17.54 |
| 2 | 400 | 0.014 | 0.4 | 12.18 | 11.4 | 10.96 |
| 3 | 400 | 0.028 | 0.2 | 29.8 | 26.2 | 24.6 |
| 4 | 400 | 0.028 | 0.4 | 17.52 | 16.6 | 15.6 |
| 5 | 600 | 0.014 | 0.2 | 9.4 | 9.0 | 9.2 |
| 6 | 600 | 0.014 | 0.4 | 6.6 | 5.7 | 5.6 |
| 7 | 600 | 0.028 | 0.2 | 14.68 | 13.2 | 13.36 |
| 8 | 600 | 0.028 | 0.4 | 9.0 | 8.8 | 8.06 |

Table 6.1: Estimate of the Unit Cutting Force

With an increase in the cutting speed, the temperature at the cutting zone increases due to the increased rate of energy dissipation. The variation of fracture toughness with temperature is shown in figure 3.1. It can be seen that there is a significant increase in fracture toughness with an increase in temperature. The three zones marked in the figure are:

- Cleavage initiation or propagation
- Increasing shear
- Full–shear initiation or propagation

The occurrence of increase in temperature and increase in loading rate at the same time marks two opposing trends for the fracture toughness. The interaction between these two effects is shown in figure 6.2. In the figure, the four curves shown are the variation of $K_{IC}$ with the temperature at four different loading

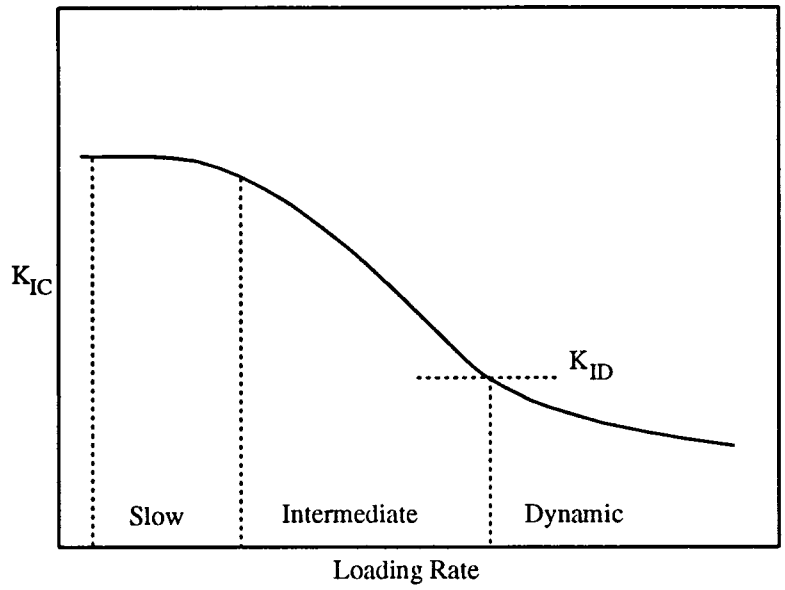


Figure 6.1: Variation of Fracture Toughness with Loading Rate[BR87]

rates. The points marked on these curves represent progressively increasing cutting speeds. The simultaneous increase in both temperature as well as the loading rate can thus cancel each other to a large extent, rendering the fracture toughness roughly constant with changing cutting speed. This causes the cutting force to be constant with changing cutting speed and explains this difference between ceramic materials and conventional materials.

A very important implication of this observation is that the traditional method of using high cutting speeds for making finish cuts may not be valid in the case of ceramic materials.

### 6.1.2 Surface and Sub-surface Damage

In the machining of ductile materials, surface and sub-surface damage do not play a very important role since the material can undergo localized plastic deformation, at the points of high stress concentrations. In ceramic materials, however,

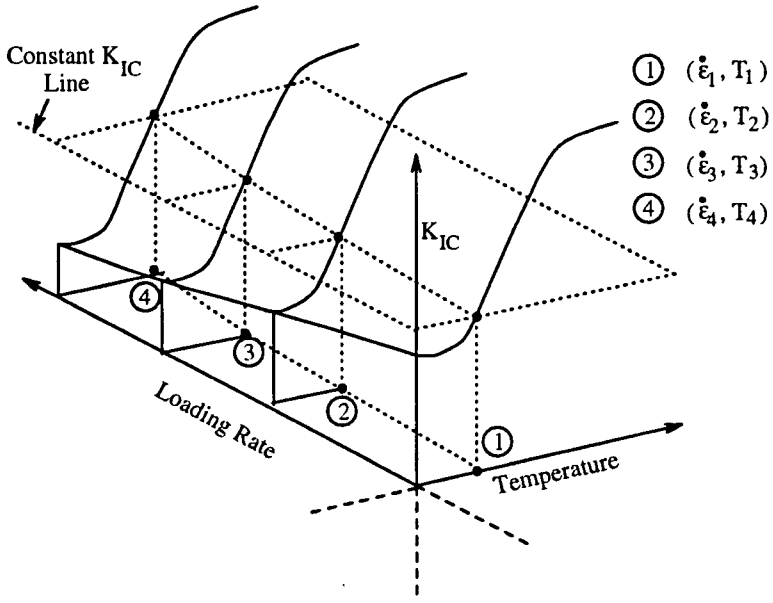


Figure 6.2: Interaction Between Temperature and Loading Rate

stress concentration at flaw locations may initiate cracks that can severely limit the performance of the component. Therefore, in the machining of ceramic materials, a study of the tendency of the process to induce damage on and below the surface is extremely essential. The effect of the initial stress distributions in the material was discussed in section 3.2. The scratch test gave physical values of the forces that are generated at the interface of the specimen and indenter, under varying depths of cut. The results of the scratch test are illustrated in figures 5.4 and 5.5. The friction factor at any instant was computed as,

$$\mu = \frac{F_x}{F_z} \tag{6.1}$$

It was discovered that there is a very significant effect of lubrication on the friction factor. While the dry friction coefficient was around 0.5, the lubricated friction coefficient fell to about 0.2. Two trials each for the cases of dry and lubricated conditions are shown in figures 5.4 and 5.5. Since a varying depth


Figure 6.3: ESEM Micrograph of a Typical Scratch Surface

of cut is used for these tests, the forces $F_x$ and $F_z$ are continuously increasing. The line of best fit has a slope that corresponds to the rate of change of the force with changing depth of cut. The values clearly indicate that there is a decrease in the slope of $F_z$ from the dry to the lubricated case. This result, coupled with the observations from the finite element analysis in section 3.2, shows that the shape of the stress field is very different in the two cases considered. An analysis of the resulting stress field is presented in section 6.2.1.

The resultant force experienced by the indenter was computed from the forces in two directions. A typical result is plotted in figure 6.4. It can be seen that the slopes of these plots are almost equal. This shows that though the friction factor changes with the application of lubricant, the resultant force remains almost unchanged. The differences in loading conditions do not affect the overall force

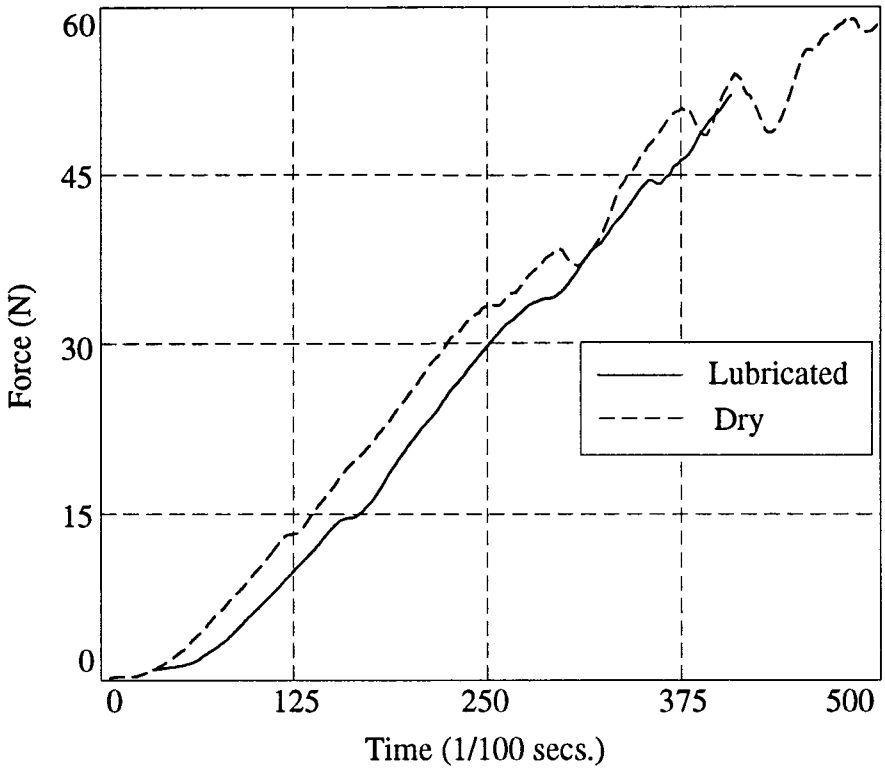


Figure 6.4: Variation of Resultant Force with Depth of Cut

required to fracture the material and move forward making a scratch. This result is consistent with the observations in the case of alumina as well as Dicor/MGC where the change in environmental conditions effected a change only in the friction factor but not in the resultant force. This suggests that the total force needed is determined by the energy required to fracture the material and form the new surface and not the environmental conditions[A.A20].

### 6.1.3 Evidence of Brittle Fracture

The chip fragments collected from the second set of experiments were analyzed under the ESEM for clues to the chip formation process. Chip fragments that have undergone plastic deformation contain parallel tracks on the surface that


Figure 6.5: ESEM Micrograph of Plastic Chip

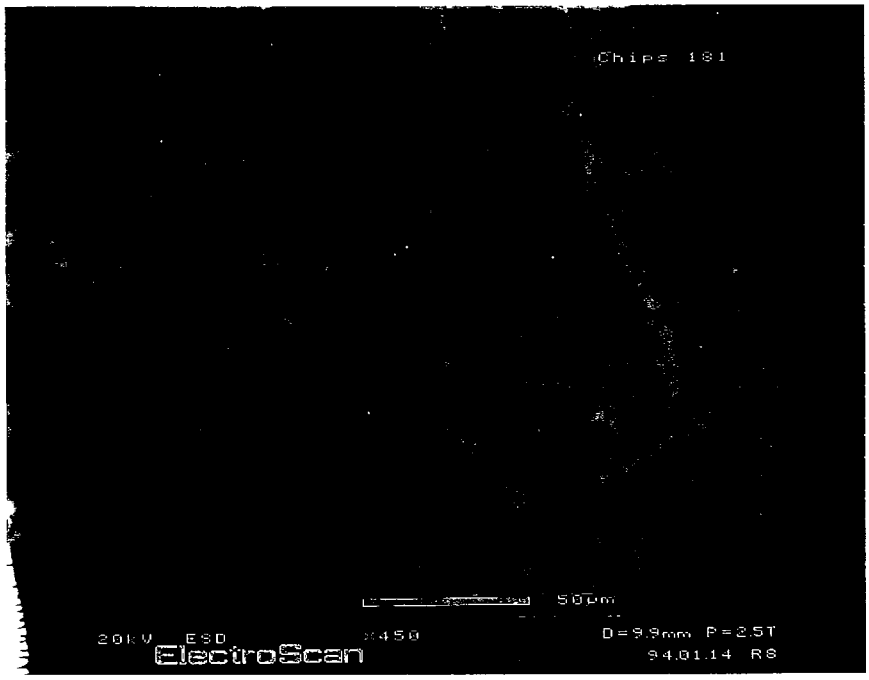


Figure 6.6: ESEM Micrograph of Chip with Arrested Crack

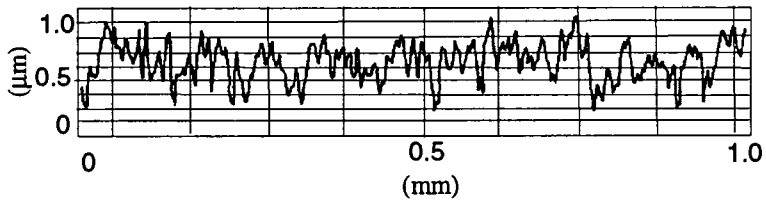


Coolant = Off $R_a = 0.275\mu m$

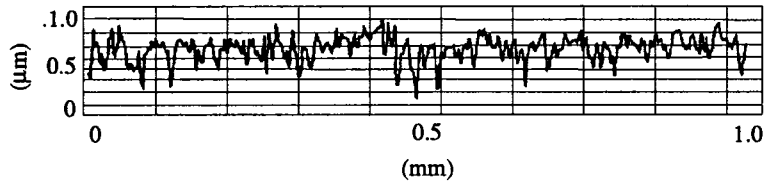


Coolant = On $R_a = 0.195\mu m$

(Feed = $0.2\frac{in}{min}$; Speed = $400rpm$; DOC = $0.0029in$; Tool = $CC$)

Figure 6.7: Surface Analysis of Two Test Specimens

was in contact with either the tool or the workpiece. It was discovered that the incidence of plastic flow was very small since such chips were very few in number. On the other hand, many chip fragments showed evidence of an arrested crack (figures 6.5 and 6.6). In addition, an overwhelming majority of the chip fragments had surfaces that were typical of brittle fracture. These give a strong indication that brittle fracture is the more significant mechanism involved in the production of chips. This substantiates the previous findings from the machining of alumina.

Further evidence of brittle fracture being the dominant mechanism of material removal was obtained from observation of the surface profiles of the machined

specimens. Two typical profiles are shown in figure 6.7. It can be seen that there is no significant trace of regularity. In the case of ductile materials, the moving tool leaves marks that are dominated by one or a few frequency components characterized by the tool geometry and the cutting parameters. The absence of such a set of frequencies suggests that the surface is generated by brittle fracture and not plastic flow.

## 6.2 Factors Influencing Material Removal

### 6.2.1 Chemo-mechanical Effects

From the results of the surface analysis of specimens machined in a submerged state, it is apparent that there is an effect of the environmental conditions on the machining performance. The fact that submerged machining reduces the sensitivity of the surface roughness value to the cutting speed further indicates that there is a change in the machining performance. To study this effect and get an understanding of the mechanisms involved, the technique of analyzing the stress field before fracture, that was used in section 3.2, was adopted. Forces obtained from the cutting force experiments were used to determine a typical loading condition. The stress distributions shown in figures 6.8 and 6.9 show that there is a dramatic change in the shape of the stress field in the two different cases of loading. There is correspondingly a change in the characteristics of the material removal process and the surface generated in the two cases can be expected to be different. In the case of greater friction force, the workpiece experiences a tensile stress in a thin layer causing the material to separate from the main workpiece in a process resembling delamination. In the other case,

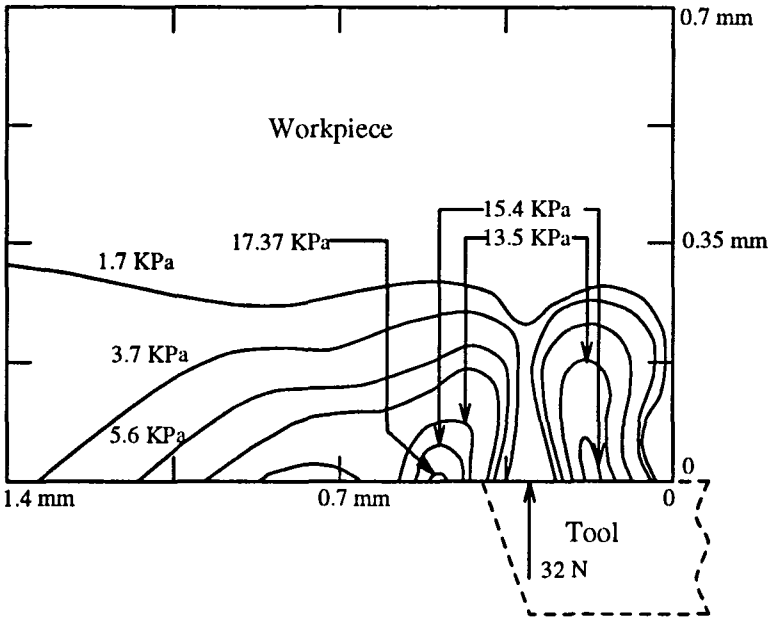


Figure 6.8: Tensile Stress Field in First Load Case

the deeper stress field causes more formation of cracks over a larger region with subsequent removal of material and residual damage.

### 6.2.2 Chemical Action of Cutting Fluid

The effect of cutting fluids on the machining process is studied through a chemical analysis of surfaces machined under varying conditions of cutting parameters. The elements chlorine and oxygen were found to change significantly and these are shown in figures 5.9 and 5.10. Using the method of orthogonal arrays, an empirical model can be built from the data. These are presented in the form of main effects and interactions. The significant factors in the models for chlorine and oxygen are listed in equations 5.1 and 5.2. These equations represent the variation of chlorine and oxygen in the machined surface. It is instructive to note that while there is an increase in the amount of chlorine upon the use of

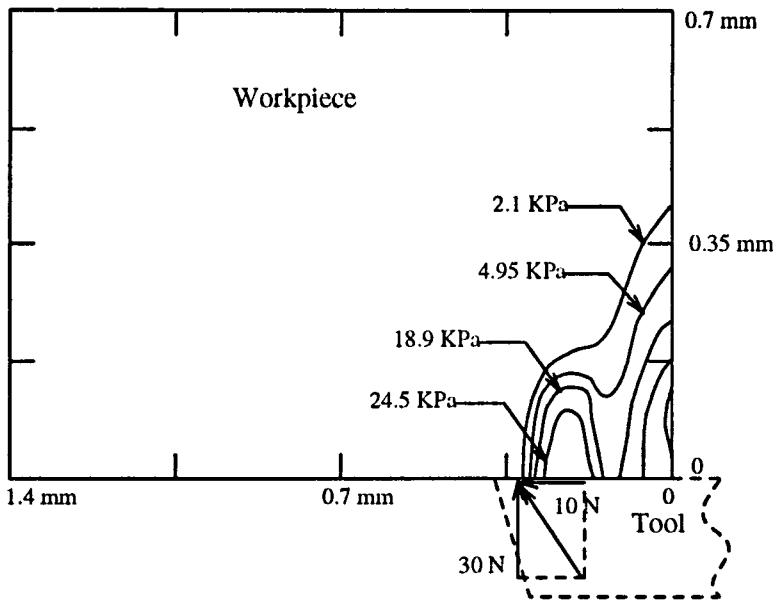


Figure 6.9: Tensile Stress Field in Second Load Case

coolant there is a decrease in the amount of oxygen. The main interactions for speed and feed are positive for chlorine, suggesting that an increase in the severity of cutting conditions causes an increase in the temperature at the tool-work interface resulting in an increase in chemical interaction.

### 6.2.3 Effect of Submerged Machining

The forces measured during the submerged machining experiments give an indication of the manner in which the application of cutting fluid affects the machining process. As can be observed from figures 5.6, 5.7 and 5.8, the forces are almost entirely dependent on the depth of cut.

The surface roughnesses of the machined specimens were measured. The results are tabulated in table 5.4. There is a marked improvement in the quality of surface from the dry case to the submerged cases. The interactions for the

| Number | Sprayed | Submerged | |
|---|---|---|---|
| | | Cold | Hot |
| 1 | 0.23 | 0.14 | 0.23 |
| 2 | 0.317 | 0.37 | 0.4 |
| 3 | 0.36 | 0.18 | 0.25 |
| 4 | 0.36 | 0.35 | 0.375 |
| 5 | 0.387 | 0.16 | 0.26 |
| 6 | 0.487 | 0.32 | 0.31 |
| 7 | 0.51 | 0.21 | 0.26 |
| 8 | 0.615 | 0.35 | 0.385 |

Table 6.2: Comparison of $R_a$ Values in Sprayed and Submerged Lubrication

variation of $R_a$ value for the three cases are listed in equations 5.5, 5.6 and 5.7. In the case of dry machining, there is a heavy dependence of $R_a$ on the cutting speed. Once again, the opposite trend of deteriorating surface quality with increase in cutting speed is substantiated. But in the cases of submerged machining, the dependence on cutting speed is reduced dramatically and feed plays the more dominant role in determining the surface quality. Futhermore, on comparison with the surface quality obtained in the case of sprayed lubrication (table 6.2), it can be seen that there is an improvement in the surface quality. This suggests that there is increased access to the cutting fluid in the case of submerged machining.

## 6.3 Factors Affecting Surface Integrity

While the maximum depth of cut achieved in the scratch test was about $70\mu m$, the low and high levels of depth of cut used for the first set of experiments were approximately 70 and $140\mu m$, respectively. Being in the same order of magnitude, it would not be unreasonable to expect the material to respond in a manner similar to the scratch tests. As expected, the application of cutting fluid resulted in an improvement in the surface finish as quantified by the surface roughness parameter $R_a$. In addition, it was observed that there was no significant effect of the change in tool material from HSS to tungsten carbide. The significant main effects and interactions are listed in equation 5.3. These were computed from the orthogonal array design of experimentation[BHH78]. This reveals the effect of the cutting fluid on the roughness value. The coefficient for *speed* is positive indicating that there is a deterioration in surface quality with increase in speed. The fact that there was almost no sign of tool wear after the 32 experiments suggested that the cutting conditions could be made more severe. This prompted the increase in depth of cut by a factor of five for the next set of experiments.

The second set of experiments showed a change in the response of the surface roughness to the cutting conditions. The significant main effects and interactions are listed in equation 5.4. The positive value for the main interaction coefficient for the speed of rotation shows the same trend as in equation 5.3. This can be clearly seen from the two surface profiles shown in figure 6.10. The two profiles are from surfaces machined under identical conditions except for the cutting speed. It is obvious that the surface machined at a high cutting speed shows a higher surface roughness. In metals, the surface roughness has been found to improve with an increase in the cutting speed. The reason for this behaviour has

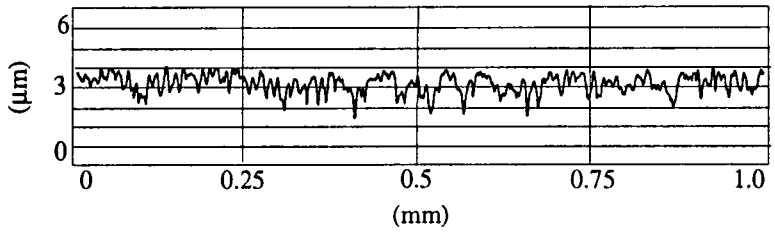


Speed = $400rpm$ $R_a = 0.36\mu m$

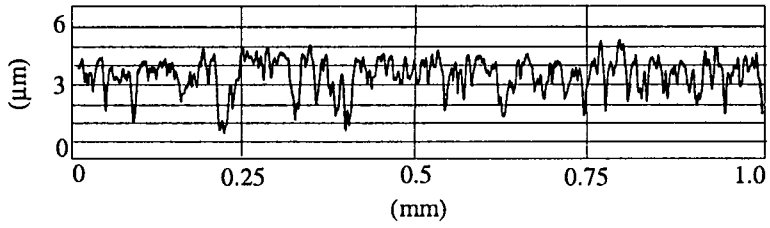


Speed = $600rpm$ $R_a = 0.615\mu m$

(Feed = $0.4\frac{in}{min}$; DOC = $0.028in$)

Figure 6.10: Comparison of the Effect of Cutting Speed

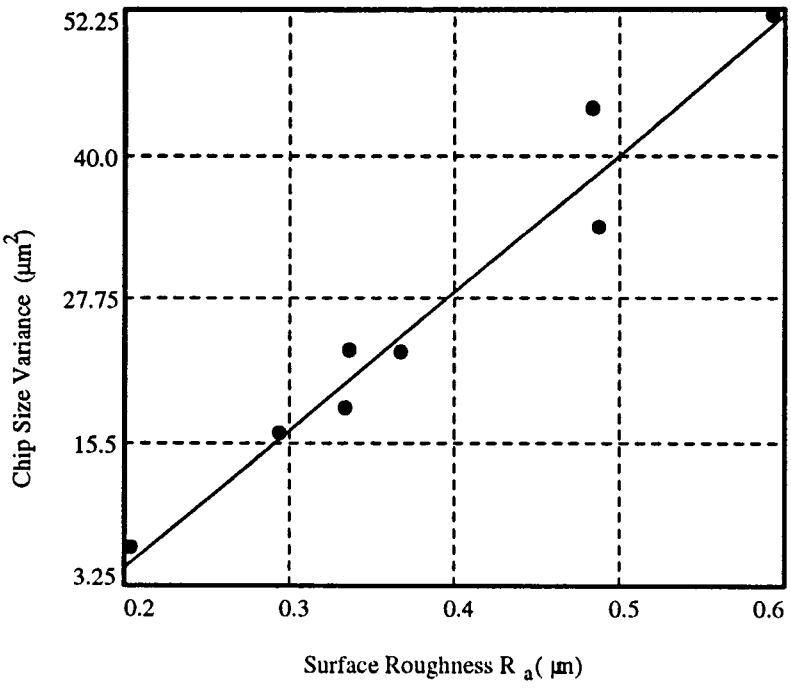


Figure 6.11: Correlation Between $R_a$ and Chip Size Variance

been determined to be the increased plasticity due to the rise in temperature at high cutting speeds. In the previous study on alumina, in six out of eight cases, the surface roughness deteriorated with the cutting speed. This suggests that this phenomenon could be due to the brittleness of the material. This further establishes that that in the machining of ceramic materials, finish cutting must not be done at very high cutting speeds.

It was discovered that there is no immediate correlation between the average chip size and the surface roughness value $R_a$. The correlation coefficient from a linear regression analysis was found to be about 0.35. On the other hand, the variation in the chip size was strongly correlated with $R_a$. The correlation coefficient in this case was found to be about 0.9. This is shown in figure 6.11. This can be understood intuitively by visualizing the machined surface as comprising

many fracture surfaces formed by chipping. As successive chip fragments forming the surface, vary in size, the variations in height produced causes a poorer surface finish. The objective of machining to realise a surface with the best $R_a$ value can, therefore, be achieved by minimising the variation in the size of chip fragments formed.

## 6.4 Guidelines to Machine Ceramics

The following guidelines are necessary to ensure quality in a machining process:

- Controlling the variation in chip size is integral to good surface finish. This can be achieved through control of the machining environment such as using cutting fluids, which may promote crack propagation, and control of the apparent coefficient of friction.

- Among material properties, the fracture toughness is a key factor regarding the material's machinability. Requirements of a large fracture toughness, which could be desirable from the designer's point of view, could render processing of the material more difficult.

- Modifications of the microstructure such as the addition of mica flakes, may balance the needs of design specifications and the machining process. Free machining steel, for instance, is the result of the inclusion of lead to improve machinability while maintaining properties of strength.

# Chapter 7

# Conclusions and Future Work

## 7.1 Conclusions

Advanced ceramic materials have become very popular due to their unique properties, such as high hardness and low thermal conductivities. Designers are employing these materials to realise new and innovative designs. However, these unique properties pose difficulties in processing the material, and present a challenge to manufacturing engineers, to improve machining quality and productivity.

This study is an investigation into the fundamental mechanisms of material removal that constitute ceramic machining. This research combines experimental and analytical work. In the experimental aspect, machining tests have been carried out to identify the effects of machining conditions on the quality of machined parts and productivity of the machining operation. In the analytical aspect, the principles of fracture mechanics have been applied to interpret the observed phenomena in hoping to gain a better understanding of the basic mechanisms of material removal, and leading to the development of new and

innovative machining technologies. The significant findings in this research are:

- The dominant mechanism of material removal in the machining of ceramics has been discovered to be brittle fracture. A five stage model has been proposed to illustrate the basic mechanism involved.

- Cutting parameters have a significant effect on the machining process. In the determination of surface quality, increase in feed or depth of cut results in a deterioration of the surface. Increase in the cutting speed, contrary to the behaviour of conventional materials, results in a poorer surface finish. It has also been observed that an increase in the feed, speed or depth of cut results in an increase in the variation in size of chips produced.

- The cutting force generated during the machining process shows little change with cutting speed. This has been explained as a result of the combined effects of increasing loading rate and increasing temperature. This result, combined with the effect of cutting speed on surface quality, shows that the traditional practice of performing finish cuts at high speed may not be extended to ceramic materials.

- The effect of the environment present during the machining process has been demonstrated to have a significant effect on the cutting process. Increased access to the cutting fluid through the process of submerged machining has been shown to improve the surface quality and alter the dependence of surface quality on the cutting parameters. The deteriorating effect of high cutting speed is subdued and the effect of feed gains greater significance.

- Control of the apparent coefficient of friction through a change in the machining environment has been demonstrated to be of vital importance in achieving micro-crack controlled machining technology.

## 7.2 Future Work

The following directions for future research in this area are suggested:

- The information and understanding gained from this study must be used in the development of a mathematical model to represent the dominant mechanisms of material removal.

- This study was limited to the machining of Dicor/MGC with a fixed microstructure. A study of the effect of microstructure on the machining efficiency needs to be performed.

- The possibility of chemical–assisted machining has been demonstrated in this study through the development of submerged machining. It is essential to study the chemical interactions that the ceramic material can undergo at raised temperatures and exploit this to improve the effectiveness of submerged machining.

- Experiments with a greater range of ceramic materials can serve to further the existing understanding about machining of ceramics.

# Appendix A

# Cutting Fluid Specifications

**Description:**

**LS-A-14H** is a versatile, heavy duty emulsifiable concentrate that can be mixed with water in ratios of 1:1 to 10:1 for metal forming operations and 5:1 to 30:1 for use in flood or mist coolant systems for machining and grinding. **LS-A-14H** is used in cutting operations on mills, turret lathes, broaches, screw machines etc., applied as a flood or mist. It is also useful on presswork - for punch forming and light drawing and for roll forming, on ferrous or non-ferrous metals.

**How To Use:**

**LS-A-14H** must be mixed by adding concentrate to water with agitation. This mixing order gives a long lasting stable emulsion in a variety of waters. Most cutting operations can be done with 5 to 30 parts water to one of concentrate. For punch press work, ratios of 1:1 to 5:1 are usually best.

**Advantages:**

| | |
|---|---|
| Density | $0.99\frac{g}{ml}$ |
| Appearance | Pale Amber Liquid |
| Odor | Mild Sweet |
| Viscosity | $550SUS \ \ 100°F$ |
| pH( 9:1 water) | $9.7 - 9.9$ |

Table A.1: Physical Characteristics

- Excellent heavy duty emulsifiable oil for a wide array of machining operations
- Reduces oil misting by as much as 95% of conventional oil based coolants
- Excellent rust protection for work in process parts
- Excellent resistance to microbial attack
- Excellent defoaming characteristics
- Excellent resistance to buildup of hard water minerals
- Contains no alkanolamines
- Leaves a soft oily non-tacky residue on parts & equipment

**Supplier:**

Tower Oil & Technology Co.

205 West Randolph Street,IL 60606

Ph: (312) 346-0562'

Fax: (312) 346-6873

# Bibliography

[A.A20] A.A.Griffith. The phenomenon of rupture and flow in solids. Philosophical Transactions of the Royal Society of London, Serial A, 221(4), 1920.

[Adv89] Advanced Materials and Processes Incorporating Metal Progress. Guide to Selecting Engineering Materials, 1989.

[A.G79] A.G.Evans. Abrasive wear in ceramics: An assessment. The Science of Ceramic Machining and Surface Finishing II, pages 1–14, 1979.

[AS76] M. Adams and G. Sines. Determination of biaxial compressive strength of a sintered alumina ceramic. Journal of the American Ceramic Society, 59(7):300–304, 1976.

[Bat89] R. C. Bates. Fracture Mechanics: microstructure and micromechanisms, chapter Micromechanical Modeling for Prediction of Lower Shelf, Transition Region, and Upper Shelf Fracture Properties. ASM International, 1989.

[Bea90] Douglas Stephen Beale. A study of the cutting mechanisms found in the machining of ceramics. Master's thesis, University of Maryland, 1990.

[BHH78] G. Box, W. Hunter, and J. Hunter. Statistics for Experimenters: An Introduction to Design, Data Analysis and Model Building. John Wiley and Sons, Inc.,, 1978.

[BR87] J. Barsom and S. Rolfe. Fracture and Fatigue Control in Structures. Prentice-Hall, 1987.

[CC91] J. Cagnoux and A. Cosculluela. Dynamic Failure of Materials: Theory, Experiment, and Numbers, chapter Influence of Grain Size on Triaxial Dynamic Behaviour of Alumina. Elsevier Applied Science, 1991.

[CJW86] Bredt Chryssolouris, G., S J., Kordas, and E Wilson. Theoretical aspects of a laser machine tool. ASME Winter Annual Meeting Proceedings, PED 20, pages 177–190, 1986.

[CK86] Joseph C. Conway and Henry P. Kirchner. Crack branching as a mechanism of crushing during grinding. Journal of the American Ceramic Society, 69(8):603–607, 1986.

[D91] Grossman. D. Structure and physical properties of dicor/mgc glass ceramic. Proceedings of the 1991 International Symposium on Computer Restorations, pages 103–115, 1991.

[EM80] A. G. Evans and D. B. Marshall. Wear mechanisms in ceramics. Fundamentals of Friction and Wear, American Society of Metals, pages 439–452, 1980.

[EW90] C. Eckert and J. Weatherall. Advanced ceramics: 90's global business outlook. Ceramics Industry, pages 53–57, 1990.

[Ger89] W. Gerberich. Fracture Mechanics: microstructure and micromechanisms, chapter The Micromechanics and Kinetics of Environmentally Induced Fracture. ASM International, 1989.

[GHK89] R. S. Gates, S. M. Hsu, and E. E. Klaus. Tribological mechanism of alumina with water. Journal of Society of Tribologists and Lubrication Engineers, 32(3):357–363, 1989.

[HC93] Kai Xiong Hu and Abijit Chandra. A fracture mechanics approach to modeling strength degradation in ceramic grinding processes. Journal of Engineering for Industry, pages 73–84, 1993.

[HM76] M Huerta and S Malkin. Grinding of glass: the mechanics of the process. Journal of Engineering for Industry, pages 459–467, 1976.

[Hwa92] T. W. Hwang. Analysis of Surface Quality in Machining of Metals and Advanced Ceramics. PhD thesis, University of Maryland, 1992.

[KBU75] W. D. Kingery, H. K. Bowen, and D. R. Uhlmann. Introduction to Ceramics. Wiley – Interscience, 1975.

[KC85] H. P. Kirchner and J. C. Conway, JR. Mechanisms of material removal and damage penetration during single point cutting of ceramics. Machining of Ceramic Materials and Components, ASME, pages 53–61, 1985.

[KCS+91] W. Konig, L. Cronjager, G. Spur, H. K. Tonshoff, M. Vigneau, and W. J. Zdeblick. Machining of new materials. Processing of Advanced Materials, pages 11–26, 1991.

[Kra91] B. Kramer. Tribological aspects of metal cutting. ASME Winter Annual Meeting Proceedings, pages 77–85, 1991.

[Law75] Brian R. Lawn. Fracture of Brittle Solids. Cambridge University Press, 1975.

[LCK85] T. J. Larchuk, J. C. Conway, and H. P. Kirchner. Crushing as a mechanism of material removal during abrasive machining. Journal of the American Ceramic Society, 68(4):209–215, 1985.

[LH89] J. Landes and R. Herrera. Fracture Mechanics: Microstructure and Micromechanisms, chapter Micromechanisms of Elastic/Plastic Fracture Toughness. ASM International, 1989.

[Maz91] M Mazurkiewicz. Understanding abrasive waterjet performance. Machining Technology, 2(1):1–3, 1991.

[Sha84] Milton C. Shaw. Metal Cutting Principles. Oxford University Press, 1984.

[SRM90] K Subramanian, S Ramanath, and Y. O. Matsuda. Precision production grinding of fine ceramics. Proceedings of the First Internation Conference on Manufacturing Technology, 1990.

[ZAGK93] G. M. Zhang, D. K. Anand, S. Ghosh, and W. F. Ko. Study of the formation of macro- and micro-cracks during machining of ceramics. Proceedings of the International Conference on Machining of Advanced Materials, pages 465–478, 1993.

[ZHAJ92] G. Zhang, T. Hwang, D. Anand, and S. Jahanmir. Tribological interaction in machining aluminum oxide ceramic. Proceedings of the Navy Tribology Workshop, Annapolis , Maryland, pages 9–13, 1992.

[ZSK94] G. Zhang, K. Satish, and W. Ko. The mechanics of material removal mechanisms in the machining of ceramics. Proceedings of the Annual Winter ASME Conference, 1994.